Sphingosine kinase 2 prevents the nuclear translocation of sphingosine 1-phosphate receptor-2 and tyrosine 416 phosphorylated c-Src and increases estrogen receptor negative MDA-MB-231 breast cancer cell growth: The role of sphingosine 1-phosphate receptor-4

Jan Ohotski[‡], Hugh Rosen[//], Robert Bittman[†], Susan Pyne,[‡] Nigel J. Pyne[‡*]

[‡]Cell Biology Group, Strathclyde Institute of Pharmacy and Biomedical Sciences, University of Strathclyde, Glasgow G4 0RE, United Kingdom

[†]Department of Chemistry and Biochemistry, Queens College, The City University of New York, Flushing, New York 11367-1597, United States

// The Scripps Research Institute, Department of Chemistry, 10550 N. Torrey Pines Rd, La Jolla, CA 92037, USA

* To whom correspondence should be addressed (n.j.pyne@strath.ac.uk)

ABSTRACT--We demonstrate that pre-treatment of estrogen receptor negative MDA-MB-231 breast cancer cells containing ectopically expressed HA-tagged sphingosine 1-phosphate receptor-2 ($S1P_2$) with the sphingosine kinase 1/2 inhibitor SKi (2-(*p*-hydroxyanilino)-4-(*p*-chlorophenyl)thiazole) or the sphingosine kinase 2 selective inhibitor (*R*)-FTY720 methyl ether (ROMe) or sphingosine kinase 2 siRNA induced the translocation of HA-tagged $S1P_2$ and Y416 phosphorylated c-Src to the nucleus of these cells. This is associated with reduced growth of HA-tagged $S1P_2$ over-expressing MDA-MB-231 cells. Treatment of HA-$S1P_2$ over-expressing MDA-MB-231 cells with the sphingosine 1-phosphate receptor-4 ($S1P_4$) antagonist CYM50367 or with $S1P_4$ siRNA also promoted nuclear translocation of HA-tagged $S1P_2$. These findings identify for the first time a signalling pathway in which sphingosine 1-phosphate formed by sphingosine kinase 2 binds to $S1P_4$ to prevent nuclear translocation of $S1P_2$ and thereby promote the growth of estrogen receptor negative breast cancer cells.

Keywords: Sphingosine 1-phosphate, Sphingosine 1-phosphate receptors, Sphingosine kinase, Cancer, Growth, Nuclear Signalling

INTRODUCTION

The bioactive lipid sphingosine 1-phosphate (S1P) is derived from the phosphorylation of sphingosine catalyzed by the two isoforms of sphingosine kinase (SK1 and SK2) and is cleaved by S1P lyase or dephosphorylated by S1P phosphatases [1-3]. S1P binds to S1P-specific G-protein coupled receptors termed $S1P_{1-5}$ and also interacts with intracellular protein targets, such as TRAF2 [1, 4]. There is now a wealth of evidence to support a role of S1P in cancer progression [5]. For instance, S1P stimulates migration of gastric tumor cells that exclusively express $S1P_3$ and inhibits the motility of others that predominantly express $S1P_2$ [6]. Similarly, the S1P-dependent inhibition of melanoma cell migration is mediated by $S1P_2$ via inhibition of Rac, activation of Rho, and tyrosine phosphorylation of focal adhesion kinase [7]. High tumor nuclear expression of both c-Src and $S1P_2$ is also associated with longer disease-specific survival time in breast cancer [8]. S1P also induces connective tissue growth factor (CTGF) expression in the Wilms' tumor cell line, WiT49, which expresses $S1P_2$ [9]. However, FTY720-phosphate, which binds to $S1P_{1/3/4/5}$, but not to $S1P_2$ [10], fails to induce CTGF expression, suggesting that the receptor involved is $S1P_2$. Indeed, S1P-stimulated CTGF expression is abolished by the $S1P_{2/4}$ antagonist JTE-013 and increased by over-expression of $S1P_2$ [9]. S1P binding to $S1P_2$ stimulates CTGF expression by the JNK- and Rho kinase-dependent pathways and CTGF expression is reduced in Wilms' tumors. In addition, over-expression of CTGF inhibits proliferation of WiT49 cells, suggesting that CTGF expression induced by $S1P_2$ is a growth inhibitor of Wilms' tumor [9].

However, $S1P_2$ has also been shown to promote cancer progression. For instance, S1P binding to $S1P_2$ increases invasiveness of glioma by a mechanism involving enhanced expression of the secreted, angiogenic matricellular protein CCN1/Cyr61 [11]. Recently, Ponnusamy et al. [12] demonstrated that systemic S1P, produced by the host SK1, promotes lung colonization and metastasis by a mechanism involving $S1P_2$. The reduction in systemic S1P inhibits TRAMP-

induced prostate cancer growth in $TRAMP^{+/+}Sk1^{-/-}$ mice or lung metastasis of various cancer cells in $Sk1^{-/-}$ mice. SK1 loss promotes the expression of breast carcinoma metastasis suppressor 1 (Brms1), and S1P binding to $S1P_2$ reduces Brms1 expression in these cancer cells [12]. Binding of S1P to $S1P_2$ induces phosphorylation of ERM proteins, which is linked with filopodia formation in cancer cells [13]. SK1/S1P has also been shown to enhance Bcr-Abl1 protein stability via a $S1P_2$-dependent mechanism [14]. In this mechanism, S1P formed by SK1 is released to act on $S1P_2$, which inactivates PP2A and thereby prevents Bcr-Abl1 degradation [14]. Therefore, the precise role of $S1P_2$ in cancer remains controversial.

We have reported that high tumor $S1P_4$ expression is associated with shortened disease-specific survival and recurrence times in patients with estrogen receptor negative tumors [15]. High $S1P_4$ expression is also correlated with node positive status, suggesting a role for this receptor in metastasis. Therefore, $S1P_4$ is an important biomarker for prognostic outcome in estrogen receptor negative breast cancer [16], providing a strong rationale for targeting this receptor with new chemotherapeutic anti-cancer agents. We have also reported that human epidermal growth factor receptor 2 (HER2)/ErbB2 functionally interacts with $S1P_4$ in estrogen receptor negative MDA-MB-453 breast cancer cells [17]. S1P binding to $S1P_4$ stimulates activation of ERK-1/2, which involves transactivation of HER2 [17]. The functional interaction of $S1P_4$ with this oncogene provides additional evidence that $S1P_4$ plays an important role in estrogen receptor negative breast cancer progression.

We demonstrate here that SK2 and S1P/$S1P_4$ normally functions to prevent nuclear translocation of $S1P_2$. These findings represent a hitherto unidentified functional interaction between SK2 and $S1P_4$ and demonstrate that the sub-cellular distribution of $S1P_2$ has a critical impact on cancer cell

growth. These findings might account for some of the conflicting reports about the function of $S1P_2$ in cancer.

MATERIALS AND METHODS

All biochemicals were from Sigma-Aldrich (Poole, UK). Anti-HA, anti-Src, and anti-GAPDH antibodies were from Santa Cruz Biotechnology (California, USA). Anti-actin and conjugated anti-IgG secondary antibodies were from Sigma (Poole, UK). Anti-phospho-Src (Y416) and anti-Lamin A/C antibodies were from Cell Signalling Technology (Massachusetts, USA). S1P was from Avanti Polar Lipids (Alabaster, AL, USA). SKi ((2-(*p*-hydroxyanilino)-4-(*p*-chlorophenyl)thiazole)) was from Merck Biosciences (Nottingham, UK). CAY10444 was from Cayman Chemical (Michigan, USA). JTE-013 was from Tocris Bioscience (Abingdon, UK). ROMe, RB-005, and 55-22 were synthesized as described previously [18-20].

Cell Culture--MDA-MB-231 was purchased from ATCC. The breast carcinoma MCF-7 cell line was a gift from Dr Rachel Schiff (Baylor College of Medicine, TX, USA). Cells were cultured in high-glucose Dulbecco's modified Eagle's medium (Invitrogen, Paisley, UK) supplemented with 10% (v/v) European fetal calf serum (Seralab, West Sussex, UK), 100 U/ml penicillin G sodium, and 10 μg/ml streptomycin sulfate (Pen-Strep, Gibco, Paisley, UK). Cells were maintained at 37 ^{o}C in 95% air and 5% CO_2. All compounds were used at 10 μM, except for S1P, which was used at 5 μM. After transfection for 24 h, the compounds were added for 4 h. S1P was added after 3 h and the duration of stimulation was 1 h.

siRNA Treatment--Cellular expression of SK1, SK2, $S1P_3$, and $S1P_4$ was reduced using sequence-specific siRNAs. Scrambled siRNA was used as a control. Cells were transfected with 100 nM siRNA prepared in culture medium containing the DharmaFECT 2 reagent (Invitrogen, Paisley,

UK). The cells were transfected for 24 h and then serum starved for 24 h prior to treatment with the compounds.

Transfection--Cells at 80% confluence were transiently transfected with either HA-$S1P_2$ construct or pcDNA3.1 vector. Cells were incubated in serum-free high-glucose Dulbecco's modified Eagle's medium and transfected using Lipofectamine 2000 (Invitrogen, Paisley, UK) according to the manufacturer's instructions. After a 24 h incubation, the cell culture medium was replaced with serum-free high glucose Dulbecco's modified Eagle's medium prior to treatment with the compounds.

Cell Lysate Preparation--Cells were harvested in SDS-PAGE sample buffer containing 125 mM Tris/HCl (pH 6.7), 0.5 mM $Na_4P_2O_7$, 1.25 mM EDTA, 50 mM DTT, 0.5% (w/v) sodium dodecyl sulfate, 0.06% (w/v) bromophenol blue, and 1.25% (v/v) glycerol.

Nuclei Preparation--Cells were scraped in 4 ml of phosphate buffered saline (PBS). The cell suspensions were transferred into 15-ml centrifuge tubes and pelleted at 700×g for 5 min. Cell nuclei were isolated using the FractionPREP Cell Fractionation kit (BioVision, California, USA). Nuclei preparations were mixed with SDS-PAGE sample buffer and processed for western blotting.

Western Blotting--Proteins were separated using SDS-PAGE and transferred to a hybond ECL nitrocellulose membrane (GE Healthcare, Buchinghamshire, UK). Membranes were blocked in 2% (w/v) bovine serum albumin (BSA) (Thermo Fisher Scientific, Massachusetts, USA) in TBST buffer (20 mM Tris/HCl (pH 7.5), 48 mM NaCl, and 0.1% (v/v) Tween 20) for 1 h at room temperature. Primary antibody was diluted in TBST buffer and incubated with membranes for 24

h at 4°C. HRP-conjugated anti-mouse or rabbit antibodies diluted in TBST buffer were used to detect the primary antibody. Membranes were incubated with secondary antibody for 1 h at room temperature. A luminol-based enhanced chemiluminescence method was used to visualize the immunoreactive protein bands.

Densitometry--Densitometric analysis of western blots was performed using ScanImage (Scion Corporation, MD, USA). Unpaired Student's t-test was used for statistical analysis.

RT-PCR--Total RNA was isolated from MDA-MB-231 cells using ISOLATE II RNA mini kit (Bioline Reagents, London, UK), according to the manufacturer's instructions. cDNA was synthesized from extracted RNA using BioScript (Bioline Reagents, London, UK). The polymerase chain reaction was used to determine the expression levels of SK1, SK2, $S1P_3$, and $S1P_4$. The following primers were used: GAPDH (forward: TGAAGGTCGGAGTCAACGGATTTGGC, reverse: CATGTGGGCCATGAGGTCCACCAC), SK1 (forward: CTGTCACCCATGAACCTGCTGTC, reverse: CATGGCCAGGAAGAGGCGCAGCA), SK2 (forward: GCCTACTTCTGCATCTACACCTACC, reverse: GAGGTTGAAGGACAGCCCAGCTTC), $S1P_3$ (forward: GACTGCTCTACCATCCTGCCC, reverse: GTAGATGACCGGGTTCATGGC) and $S1P_4$ (forward: GGCACAGCCGGCTCATTGTT, reverse: AAGCTGAGCACGGCTCTGCACA). Amplification reactions were for 30 cycles, starting with denaturation for 30 s at 94 °C, annealing for 1 min at 56 °C, and extension for 1 min at 72 °C, performed using the ABI Model 7300 PCR machine.

xCELLgence Assay--The growth of MDA-MB-231 cells was monitored using the xCELLigence system. Cells were plated in 96 wells E-plates (Acea Biosciences, CA, USA) and incubated for 24

h at 37°C. Cells were transfected for 24 h as described before, and the cell culture medium was changed prior to treatment with the compounds for 4 h. After S1P was added after 3 h, the cells were incubated for 1 h. Cell index was measured and recorded using the xCELLigence software (Acea Biosciences, CA, USA).

RESULTS

Effect of SK1/SK2 Inhibitor on $S1P_2$ Subcellular Localization--First, we established the sub-cellular distribution of ectopically expressed HA-tagged $S1P_2$ (HA-$S1P_2$) in estrogen receptor negative MDA-MB-231 breast cancer cells. HA-$S1P_2$ was present in nucleus of untreated cells (Fig. 1A) and migrated on SDS-PAGE as two immunoreactive protein bands that sometimes are smeared, indicative of post-translation modification, e.g. glycosylation. There is, in fact, substantial evidence demonstrating that GPCRs, including $S1P_1$, are localized in the nucleus of cells [21-23] and that the nuclear lysophosphatidic acid receptor-1 (LPA_1) can induce PI3K-mediated signalling to regulate inflammatory gene expression [24, 25].

We next investigated whether SK regulates the nuclear localization of HA-$S1P_2$. Surprisingly, pre-treatment of MDA-MB-231 cells with the SK1/2 inhibitor, SKi increased the amount of HA-$S1P_2$ in the nucleus by 150 % (Fig. 1A, Suppl Fig. 1). SKi had no effect on the total expression level of HA-$S1P_2$ in MDA-MB-231 cells (Fig. 1B). This excludes changes in expression of HA-$S1P_2$ as a possibility that might have accounted for the increase in nuclear HA-$S1P_2$ levels in response to SKi. Therefore, SK normally functions to prevent the nuclear localization of $S1P_2$. We also found that Y416 phosphorylated c-Src was present in the nucleus and that treatment of cells with SKi increased the amount of this phosphorylated protein in the nucleus (Fig. 1A, and Suppl Fig. 1). Treatment of HA-$S1P_2$ over-expressing MDA-MB-231 cells with S1P reduced the amount of HA-$S1P_2$ and Y416 phosphorylated c-Src that accumulates in the nucleus in response to SKi (Fig. 1A, Suppl Fig. 1). The nuclear localization of Y416 phosphorylated c-Src has been reported before [26], and has been shown to induce export of the anti-oxidant protein Nrf2 to the cytoplasm where it is degraded by the proteasome [26]. However, we were unable to detect nuclear export of Nrf2 in response to SKi (data not shown).

Treatment of MDA-MB-231 over-expressing HA-$S1P_2$ with SKi failed to increase the phosphorylation of c-Src on Y416 above basal levels, detected in whole cell lysates (Fig. 1B, Suppl Fig. 2). This suggests that SK normally suppresses the translocation of a small pool of c-Src that is phosphorylated on Y416 to the nucleus. Furthermore, treatment of vector-transfected MDA-MB-231 cells (that lack ectopically expressed HA-$S1P_2$) with SKi promoted the nuclear translocation of c-Src that was not phosphorylated on Y416 (Fig. 1C, Suppl Fig. 3). This contrasts with MDA-MB-231 cells expressing HA-$S1P_2$, where the Y416 phosphorylated form of c-Src accumulates in the nucleus in response to SKi, and this therefore appears dependent on the presence of HA-$S1P_2$.

In addition, SK, $S1P_2$, and Y416 phosphorylated Src do not functionally interact in estrogen receptor positive MCF-7 cells over-expressing HA-$S1P_2$. Thus, SKi failed to promote an increase in the nuclear content of HA-$S1P_2$ or Y416 phosphorylated c-Src in these cells (Fig. 1D, Suppl Fig. 4). This suggests that the presence of the estrogen receptor might prevent the functional interaction between SIP_2 and SK.

SK2 Regulates the Nuclear Translocation of HA-$S1P_2$ and Y416 Phosphorylated c-Src--We next investigated whether the nuclear localization of HA-$S1P_2$ and Y416 phosphorylated c-Src is regulated by SK1 or SK2 or both. For this purpose, we used the SK1-selective inhibitors, 55-22 and RB-005, both of which failed to mimic the effect of SKi in promoting the nuclear translocation of HA-$S1P_2$ and Y416 phosphorylated c-Src in HA-$S1P_2$ over-expressing MDA-MB-231 cells (Fig. 2A, B, Suppl Fig. 5A, B). Moreover, siRNA knockdown SK1 failed to induce the nuclear accumulation of HA-$S1P_2$ and Y416 phosphorylated c-Src in these cells (Fig. 2C, Suppl Fig. 5C).

The treatment of HA-$S1P_2$ over-expressing MDA-MB-231 cells with the SK2-selective inhibitor (*R*)-FTY720 methyl ether (ROMe) or siRNA knockdown of SK2 induced the nuclear accumulation of HA-$S1P_2$ and Y416 phosphorylated c-Src (Fig. 1C, Fig. 2D, E, Suppl Fig. 5D, E). Furthermore, treatment of these cells with S1P reduced the amount of HA-$S1P_2$ in the nucleus in response to ROMe but not SK2 siRNA (Fig. 2D, Suppl Fig. 5D). ROMe did not increase the phosphorylation of c-Src on Y416, and had no effect on HA-$S1P_2$ expression levels in whole cell lysates (Fig. 2F, Suppl Fig. 6). The latter finding excludes changes in expression of HA-$S1P_2$ as a possibility that might have accounted for the increase in nuclear HA-$S1P_2$ levels in response to ROMe. In contrast with SKi, S1P failed to reverse the effect of ROMe or SK2 siRNA on the translocation of Y416 phosphorylated c-Src (Fig. 2D, E, Suppl Fig. 5D, E).

Influence of $S1P_4$ on the Nuclear Translocation of $S1P_2$ and Y416 Phosphorylated c-Src--The ability of exogenous S1P to prevent the SKi- and ROMe-induced nuclear translocation of HA-$S1P_2$ suggests a role for other S1P receptors in regulating the localization of $S1P_2$ in these cells. For instance, SK2 might be functionally linked with S1P receptors by producing S1P that can be released ('inside-out' signalling) from the cells to bind to these receptors and prevent nuclear accumulation of HA-$S1P_2$. Therefore, we used pharmacological sub-type selective S1P receptor antagonists and siRNA approaches to establish the effect of other S1P receptors on the nuclear translocation of HA-$S1P_2$ and Y416 phosphorylated c-Src in MDA-MB-231 cells. In this regard, the $S1P_{2/4}$ antagonist JTE-013 [17, 27], the $S1P_3$ antagonist CAY10444 [28], or $S1P_3$ siRNA had no effect on the nuclear accumulation of HA-$S1P_2$ and Y416 phosphorylated c-Src (Fig. 3A-C, Suppl Fig. 7A-C). However, the $S1P_4$ antagonist CYM50367 [29] promoted the accumulation of HA-$S1P_2$, but not Y416 phosphorylated c-Src, in the nucleus (Fig. 3D, Suppl Fig. 7D). In addition, exogenous S1P, which can compete with CYM50367 for $S1P_4$, reduced the amount of HA-$S1P_2$ in the nucleus in response to CYM50367 (Fig. 3D, Suppl Fig. 7D). siRNA knockdown

of $S1P_4$ also recapitulated the effect of CYM50367 in promoting the accumulation of HA-$S1P_2$ in the nucleus (Fig. 3E, Suppl Fig. 7E). siRNA knockdown of $S1P_4$ had no effect on HA-$S1P_2$ expression in whole cell lysates (Fig. 3F), thereby excluding changes in expression of HA-$S1P_2$ as a possibility that might have accounted for the increase in nuclear HA-$S1P_2$ levels in response to $S1P_4$ siRNA.

Interestingly, S1P was unable to reduce the amount of HA-$S1P_2$ that accumulated in the nucleus in response to $S1P_4$ siRNA (Fig. 3E, Suppl Fig. 7E), suggesting that the inhibitory effect of S1P on the nuclear accumulation of HA-$S1P_2$ is mediated by $S1P_4$. Therefore, these results demonstrate that $S1P_2$ translocation to the nucleus is regulated by an autocrine loop involving S1P and $S1P_4$. In contrast, the translocation of Y416 phosphorylated c-Src to the nucleus appears to be regulated by a mechanism that does not involve $S1P_3$ or $S1P_4$.

Role of Nuclear Translocation of $S1P_2$ and Y416 Phosphorylated c-Src in Regulating MDA-MB-231 Cell Growth--We next investigated the effect of over-expressing HA-$S1P_2$ on the growth of MDA-MB-231 cells treated with the various inhibitors or siRNA knockdown of SK1 or SK2. Treatment of HA-$S1P_2$ over-expressing MDA-MB-231 cells with SKi, ROMe, CYM50367, or SK2 siRNA induced a reduction in growth; this effect was stronger compared with the effect of these compounds or SK2 siRNA in vector-transfected MDA-MB-231 cells (Fig. 4). JTE-103, CAY10444, SK1 siRNA, 55-22, and RB-005 reduced growth, but there was no discernible difference between HA-$S1P_2$ or vector-transfected cells (Fig. 4). These findings are consistent with the possibility that SK2 but not SK1 or $S1P_3$ limits translocation of $S1P_2$ and Y416 phosphorylated c-Src to the nucleus to promote the growth of MDA-MB-231 cells.

DISCUSSION

A model for the functional interaction between $S1P_4$, $S1P_2$, SK2 and Y416 phosphorylated c-Src in estrogen receptor negative breast cancer cells is shown in Fig. 5. Our findings suggest a role for S1P formed by SK2, which binds to $S1P_4$ to prevent nuclear translocation of $S1P_2$ and to promote the growth of estrogen receptor negative breast cancer cells (Fig. 5A). One possible model might involve heterodimerisation of $S1P_2$ and $S1P_4$ at the plasma membrane in response to S1P and which would prevent translocation of $S1P_2$ to the nucleus. Production of S1P by SK2 or exogenously added S1P would maintain this state, while inhibition of SK2 might induce dissociation due to reduced S1P levels; enabling $S1P_2$ to move to the nucleus. Indeed, exogenously added S1P reverses the effect of SKi or ROMe on the nuclear translocation of HA-$S1P_2$, and this is likely mediated by activation of $S1P_4$. Surprisingly, S1P failed to reverse the effect of SK2 siRNA, although it is possible that knockdown of SK2 might affect $S1P_4$ expression. Further studies are necessary to establish if this is indeed, the case. There is a precedent, as we have shown that siRNA knockdown of SK1 reduces $S1P_3$ expression in MCF-7 cells [30].

SK2 also prevents the nuclear translocation of Y416 phosphorylated c-Src and this appears to be independent of $S1P_4$ and might involve an intracellular S1P-dependent mechanism, which is resistant to exogenously added S1P (Fig. 5B). However, exogenously added S1P did block the effects of SKi on nuclear translocation of Y416 phosphorylated c-Src. Therefore, the effects of SKi are not fully recapitulated by ROMe and suggest that additional unidentified mechanisms might operate to regulate the translocation of Y416 phosphorylated c-Src to the nucleus in response to SKi.

The novel pathways identified here represent a therapeutic target for intervention in estrogen receptor negative breast cancer. This is specifically aimed at abrogating the function of $S1P_4$ and

SK2 to promote nuclear translocation of $S1P_2$ and Y416 phosphorylated c-Src and to therefore reduce the growth of estrogen receptor negative breast cancer cells.

REFERENCES

1. S. Pyne, N.J. Pyne, Biochem. J. 349 (2000) 385-402.
2. K. Takabe, S.W. Paugh, S. Milstien, S. Spiegel, Pharmacol Rev. 60 (2008) 181-195.
3. H. Rosen, P.J. Gonzalez-Cabrera, M.G. Sanna, S. Brown, Annu Rev Biochem.78 (2009) 743-768.
4. S.E. Alvarez, K.B. Harikumar, N.C. Hait, J. Allegood, G.M. Strub, E.Y. Kim, M. Maceyka, H. Jiang, C. Luo, T. Kordula, S. Milstien, S. Spiegel, Nature 465 (2010) 1084-1088.
5. N.J. Pyne, S. Pyne, Nature Rev. Cancer 10 (2010) 489-503.
6. H. Yamashita, J. Kitayama, D. Shida, H. Yamaguchi, K. Mori, M. Osada, S. Aoki, Y, Yatomi, Y. Takuwa, H. Nagawa, Surg. Res. 130 (2006) 80-87.
7. K. Arikawa, N. Takuwa, H. Yamaguchi, N. Sugimoto, J. Kitayama, H. Nagawa, K. Takehara, Y. Takuwa, J. Biol. Chem. 278 (2003) 32841-32851.
8. J. Ohotski, J. Edwards, B. Elsberger, C. Watson, C. Orange, E. Mallon, S. Pyne, N.J. Pyne, Int. J. Cancer 132 (2013) 605-616.
9. M.H. Li, T. Sanchez, A. Pappalardo, K.R. Lynch, T. Hla, F. Ferrer, Mol. Cancer Res. 6 (2008) 1649-1656.
10. W.J. Valentine, V.I. Godwin, D.A. Osborne, J. Liu, Y. Fujiwara, J. Van Brocklyn, R. Bittman, A.L. Parrill, G. Tigyi, J. Biol. Chem. 286 (2011) 30513-30525.
11. N. Young, J.R. Van Brocklyn, Exp. Cell Res. 313 (2007) 1615-1627.
12. S. Ponnusamy, S.P. Selvam, S. Mehrotra, T. Kawamori, A.J. Snider, L.M. Obeid, Y. Shao, R. Sabbadini, B. Ogretmen, EMBO Mol. Med. 4 (2012) 761-775.
13. K.A. Gandy, D. Canals, M. Adada, M. Wada, P. Roddy, A.J. Snider, Y.A. Hannun, L.M. Obeid, Biochem. J. 449 (2013) 661-672.
14. A. Salas, S. Ponnusamy, C.E. Senkal, M. Meyers-Needham, S.P. Selvam, S.A. Saddoughi, E. Apohan, R.D. Sentelle, C. Smith, C.R. Gault, L.M. Obeid, H.M. El-Shewy, J. Oaks, R.

Santhanam, G. Marcucci, Y. Baran, S. Mahajan, D. Fernandes, R. Stuart, D. Perrotti, B. Ogretmen, Blood 117 (2011) 5941-5952.

15. J. Ohotski, J.S. Long, C. Orange, B. Elsberger, E. Mallon, J. Dought, S. Pyne, N.J. Pyne, J. Edwards, Br. J. Cancer 106 (2012) 1453-1459.
16. S. Pyne, J.E. Edwards, J. Ohotski, N.J. Pyne, Frontiers of Molecular and Cellular Oncology 2 (2012) 168.
17. J.S. Long, Y. Fujiwara, J. Edwards, C.Tannahill, G.Tigyi, S. Pyne, N.J Pyne, J. Biol. Chem. 285 (2010) 35957-35966.
18. K.G. Lim, C., Sun, R. Bittman, N.J. Pyne, S. Pyne, Cell. Signal. 23 (2011)1590-1595.
19. D.J. Baek, N. MacRitchie, N.J. Pyne, S. Pyne, R. Bittman, Chem. Commun. 49 (2013) 2136-2138.
20. H-S. Byun, N. MacRitchie, S. Pyne, N.J. Pyne, R. Bittman, Med. Chem. Commun. 4 (2013) 1394-1399.
21. J.J. Liao, M.C. Huang, M. Graler, Y. Huang, H. Qiu, E.J. Goetzl, J. Biol. Chem. 282 (2007) 1964-1972.
22. B. Boivin, D. Chevalier, L.R. Villeneuve, E. Rousseau, B.G. Allen, J. Biol. Chem. 278 (2003) 29153-29163.
23. D.K. Lee, A.J. Lanca, R. Cheng, T. Nguyen, X.D. Ji, F. Gobeil Jr, S. Chemtob, S.R. George, B.F. O'Dowd, J. Biol. Chem. 279 (2004) 7901-7908.
24. F. Gobeil Jr, S.G. Bernier, A. Vazquez-Tello,S. Brault, M.H. Beauchamp, C. Quiniou, A.M. Marrache, D. Checchin, F. Sennlaub, X. Hou, M. Nader, G. Bkaily, A. Ribeiro-da-Silva, E.J. Goetzl, S. Chemtob, J. Biol. Chem. 278 (2003) 38875-38883.
25. C.M. Waters, B. Saatian, N.A. Moughal, Y. Zhao, G. Tigyi, V. Natarajan, S. Pyne, N.J. Pyne, Biochem. J. 398 (2006) 55-62.
26. S.K. Niture, A.K. Jain, P.M. Shelton, A.K. Jaiswal, J. Biol. Chem. 286 (2011) 28821-28832.

27. T. Ohmori, Y. Yatomi, M. Osada, F. Kazama, T. Takafuta, H. Ikeda, Y. Ozaki, Cardiovasc. Res. 58 (2003) 170-177.
28. Y. Koide, T. Hasegawa, A. Takahashi, A. Endo, N. Mochizuki, M. Nakagawa, A. Nishida, J. Med. Chem. 45 (2002) 4629-4638.
29. M. Urbano, M. Guerrero, J. Zhao, S. Velaparthi, M.T. Schaeffer, S. Brown, H. Rosen, E. Roberts, Bioorg. Med. Chem. Lett. 21 (2011) 5470-5474.
30. J.S. Long, J. Edwards, C. Watson, S. Tovey, K. Mair, R. Schiff, V. Natarajan, N.J. Pyne, S. Pyne, Mol. Cell. Biol. 30 (2010) 3827-3841.

ACKNOWLEDGEMENTS

This work was supported by a Breast Cancer Campaign grant to NJP and SP and NIH HL-083187 to RB. JO thanks the University of Strathclyde for a PhD scholarship. CYM50367 was discovered in the Scripps Research Institute Molecular Libraries Screening Center (MH084512 to HR).

CONFLICT OF INTEREST

The authors declare no conflict of interest.

FIGURE LEGENDS

FIGURE 1. Effects of SKi on the nuclear translocation of $S1P_2$ and Y416 phoshorylated c-Src. Vector- or HA-$S1P_2$-transfected MDA-MB-231 or MCF-7 cells were treated with SKi (10 μM) for 4 h and with S1P (5 μM) in the last 1 h. (A) Nuclei preparations were western blotted with anti-HA, anti-c-Src, anti-Y416 phosphorylated c-Src, and anti-lamin antibodies. The western blot shows the nuclear translocation of HA-$S1P_2$ and Y416 phosphorylated c-Src in response to SKi in MDA-MB-231 cells. Also shown are western blots with anti-lamin (a nuclear marker) and anti-GAPDH (a cytoplasmic marker) antibodies to verify the purity of the nuclei preparation. (B) MDA-MB-231 whole cell lysates were western blotted with anti-HA, anti-c-Src, anti-Y416 phosphorylated c-Src, and anti-actin antibodies. The western blot demonstrates that treatment of cells with SKi failed to increase the phosphorylation of c-Src on Y416 in HA-$S1P_2$-transfected and vector-transfected cells. (C) Nuclei preparations were western blotted with anti-c-Src, anti-Y416 phosphorylated c-Src, and anti-lamin antibodies. The western blot shows that that treatment of cells with SKi promotes nuclear translocation of non-phosphorylated c-Src in vector-transfected MDA-MB 231 cells. (D) Nuclei preparations of MCF-7 cells were western blotted with anti-Y416 phosphorylated c-Src and anti-lamin antibodies. The western blot shows that treatment of MCF-7 cells with SKi fails to induce the nuclear translocation of HA-$S1P_2$ and Y416 phosphorylated c-Src. These are representative results of three different preparations of cells.

FIGURE 2. Effects of SK1 and SK2 inhibitors and specific siRNA on the nuclear translocation of $S1P_2$ and Y416 phoshorylated c-Src. Vector- or HA-$S1P_2$-transfected MDA-MB-231 were treated with 55-22, RB-005, or ROMe (all at 10 μM) for 4 h and with S1P (5 μM) in the last 1 h or with scrambled or SK1 or SK2 specific siRNA according to the methods with

subsequent addition of S1P for 1 h. (A-E) Nuclei preparations were western blotted with anti-HA, anti-c-Src, anti-Y416 phosphorylated c-Src, and anti-lamin antibodies. The western blots show the failure of RB-005 (A), 55-22 (B), and SK1 siRNA (C) to induce nuclear translocation of HA-$S1P_2$ and Y416 phosphorylated c-Src. In (C), the inset shows successful knock down of SK1 mRNA with SK1 siRNA as assessed by RT-PCR analysis. (D and E) Western blots show nuclear translocation of HA-$S1P_2$ and Y416 phosphorylated c-Src in response to ROMe (D) and SK2 siRNA (E), respectively, and inhibition of the effects of ROMe with S1P (D). In (E), the inset shows successful knock down of SK2 mRNA with the SK2 siRNA as assessed by RT-PCR analysis. (F) MDA-MB-231 whole cell lysates were western blotted with anti-Y416 phosphorylated c-Src, anti-HA, and anti-actin antibodies. The western blot demonstrates that ROMe fails to increase the phosphorylation of c-Src on Y416 in HA-$S1P_2$-transfected and vector-transfected cells and has no effect on HA-$S1P_2$ expression. These are representative results of three different preparations of cells.

FIGURE 3. Effects of S1P receptor antagonists and specific S1P receptor siRNA on the nuclear translocation of $S1P_2$ and Y416 phoshorylated c-Src. Vector or HA-$S1P_2$ transfected MDA-MB-231 were treated with JTE-013, CAY10444, or CYM50367 (all at 10 μM) for 4 h and with S1P (5 μM) in the last 1 h or with scrambled or $S1P_3$ or $S1P_4$ specific siRNA according to the methods with subsequent addition of S1P for 1 h. (A-E) Nuclei preparations were western blotted with anti-HA, anti-c-Src, anti-Y416 phosphorylated c-Src, and anti-lamin antibodies. The western blots show the failure of JTE-013 (A), CAY10444 (B), and $S1P_3$ siRNA (C) to induce nuclear translocation of HA-$S1P_2$ and Y416 phosphorylated c-Src. In (C), the inset shows successful knock down of $S1P_3$ mRNA with the $S1P_3$ siRNA as assessed by RT-PCR analysis. (D and E) Western blots show nuclear translocation of HA-$S1P_2$ in response to CYM50367 (D) and $S1P_4$ siRNA (E), respectively, and inhibition of the effects of CYM50367

with S1P (D). In (E), the inset shows successful knock down of $S1P_4$ mRNA with the $S1P_4$ siRNA as assessed by RT-PCR analysis. (F) The western blot shows that $S1P_4$ siRNA has no effect on HA-$S1P_2$ expression, detected in whole cell lysates. These are representative results of three different preparations of cells.

FIGURE 4. Effects of SK1 and SK2 inhibitors, S1P receptor antagonists, and specific SK isoform siRNA on growth of MDA-MB-231 cells. Vector or HA-$S1P_2$ transfected MDA-MB-231 were treated with JTE-013, CAY10444, SKi, RB-005, 55-22, ROMe, or CYM50367 (all at 10 μM) for 4 h or with scrambled or SK1 or SK2 specific siRNA. Cell impedance index was used as a measure of cell growth. The indices were determined for each treatment (* $P < 0.05$ *versus* vector-transfected cells, $n = 3$).

FIGURE 5. Schematic showing the functional interaction between (A) SK2 and $S1P_4$ that regulates the nuclear translocation of $S1P_2$ and (B) between SK2 and nuclear translocation of Y416 phosphorylated c-Src.

ABBREVIATIONS

Bcr-Abl1, B-cell receptor-Abelson tyrosine kinase 1; Brms1, breast carcinoma metastasis suppressor 1; cyto, cytoplasmic preparation; ER, estrogen receptor; ERM, Ezrin, Radixin, Moesin protein; ERK, extracellular signal regulated kinase; GAPDH, glyceraldehyde 3-phosphate dehydrogenase; HA, Hemagluttinin; HER2, human epidermal growth factor receptor 2; Nrf2, nuclear factor-like 2; Nuc, nucleur preparation; PM, plasma membrane; PP2A, protein phosphatase 2A; ROMe, (*R*)-FTY720 methyl ether; S1P, sphingosine 1-phosphate; SKi, 2-(*p*-hydroxyanilino)-4-(*p*-chlorophenyl)thiazole; SK1, sphingosine kinase 1; SK2, sphingosine kinase 2; $S1P_2$, sphingosine 1-phosphate receptor-2, $S1P_3$, sphingosine 1-phosphate receptor-3; $S1P_4$, sphingosine 1-phosphate receptor-4.

Fig. 1A

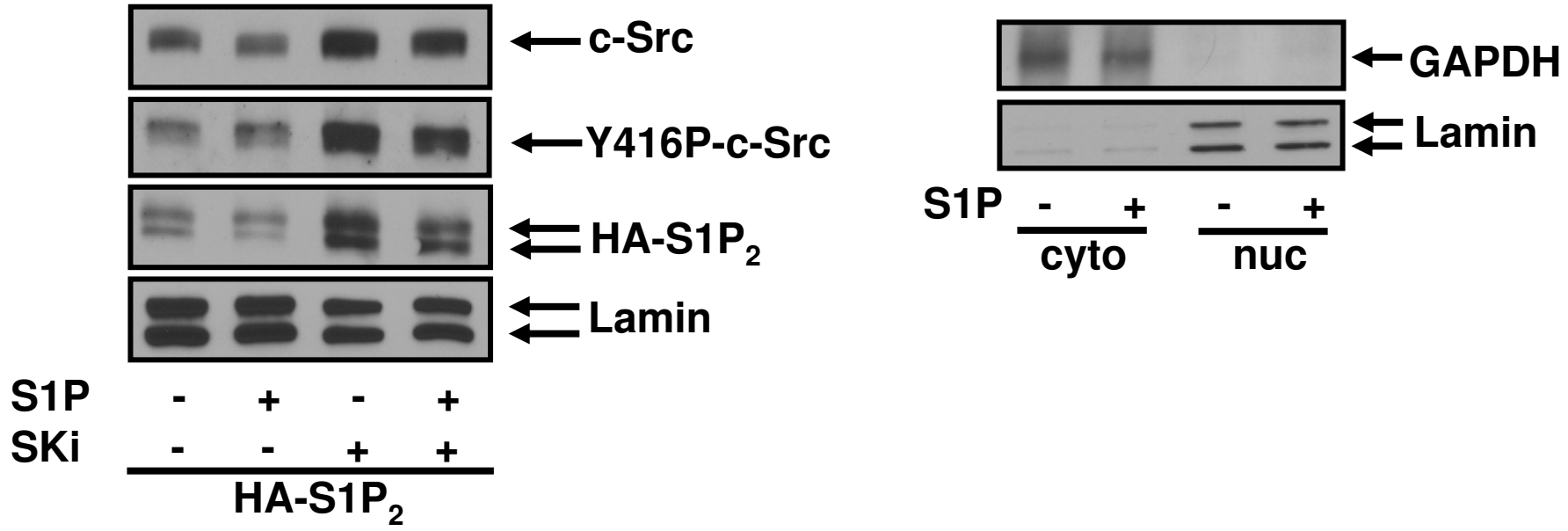
c-Src
Y416P-c-Src
HA-S1P2
Lamin
S1P - + - +
SKi - - + +
HA-S1P2
GAPDH
Lamin
S1P - + - +
cyto
nuc

Fig. 1B

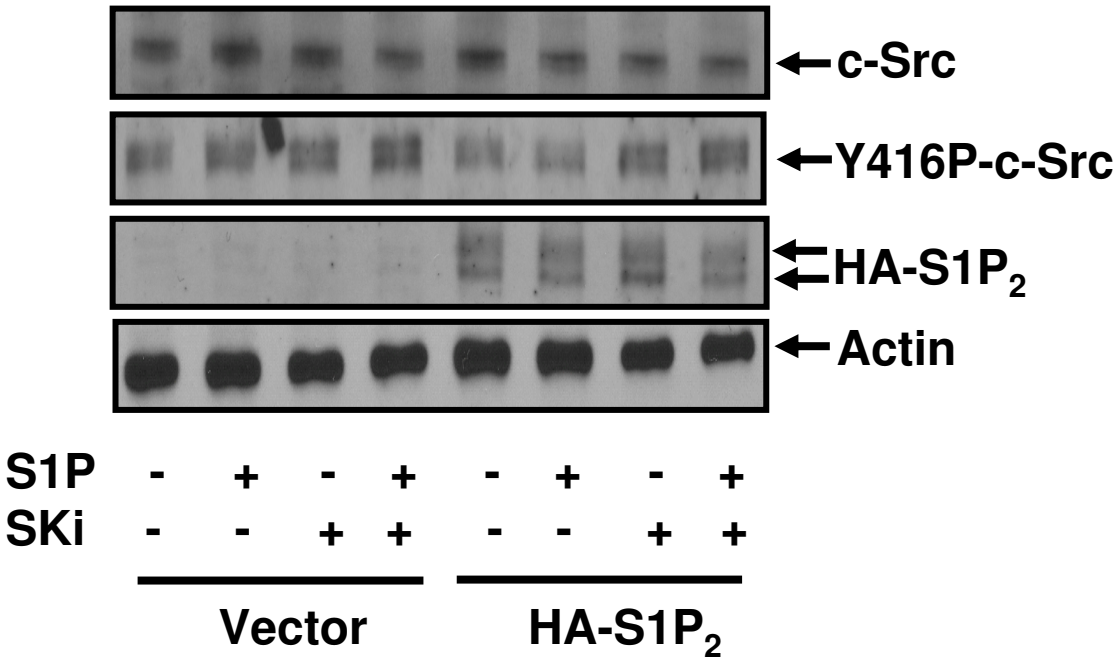
c-Src
Y416P-c-Src
HA-S1P2
Actin
S1P - + - + - + - +
SKi - - + + - - + +
Vector
HA-S1P2

Fig. 1C

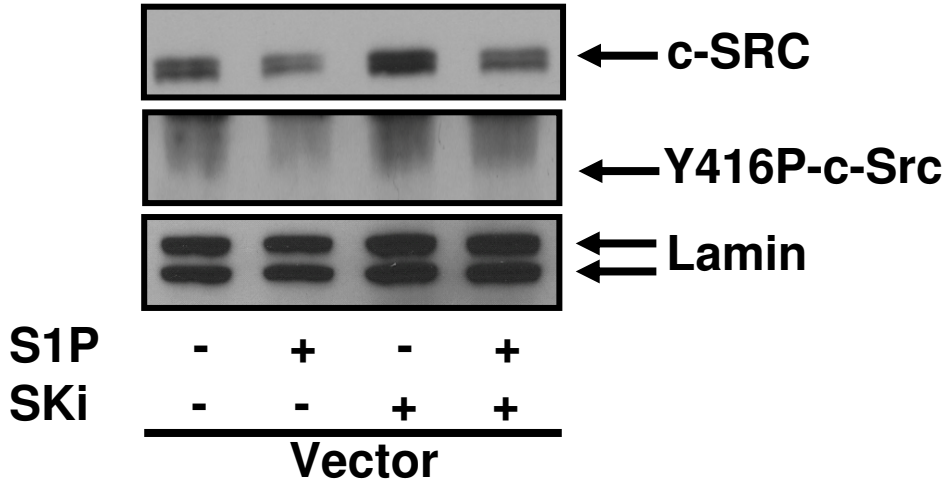
c-SRC
Y416P-c-Src
Lamin
S1P - + - +
SKi - - + +
Vector

Fig. 1D

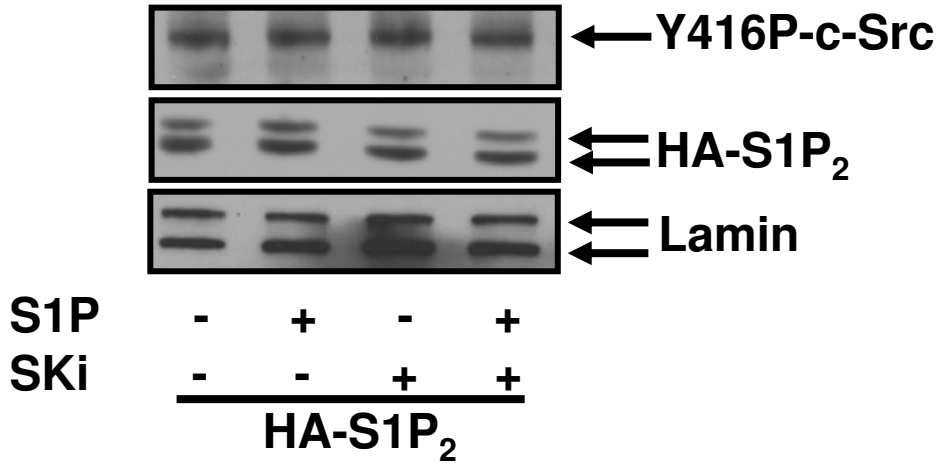
Y416P-c-Src
HA-S1P2
Lamin
S1P - + - +
SKi - - + +
HA-S1P2

Fig. 2A

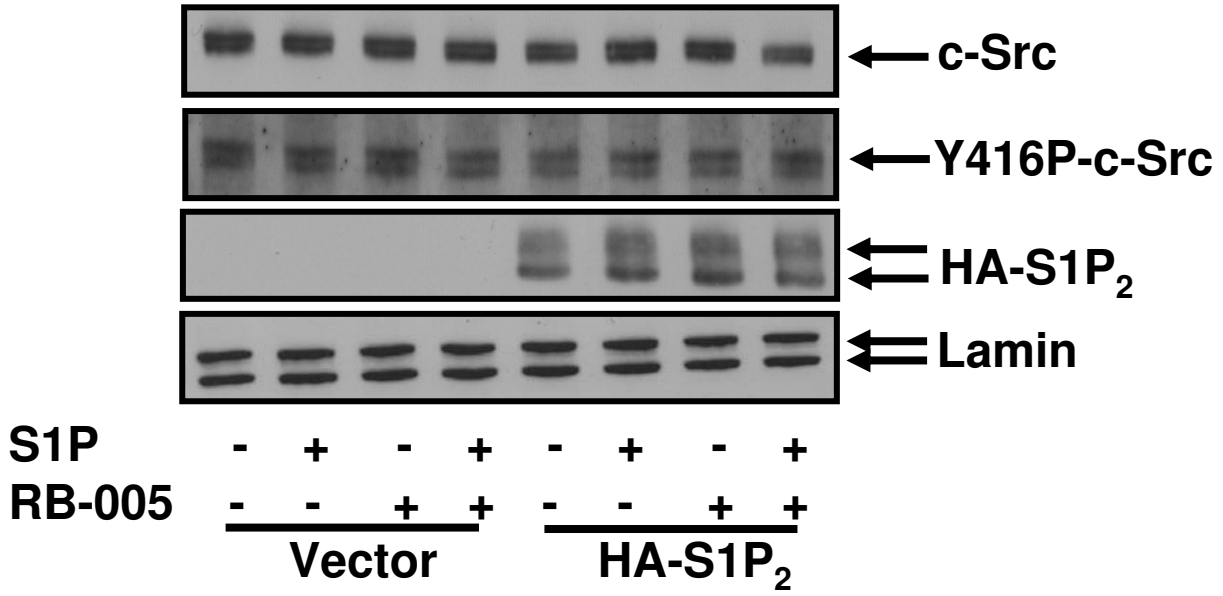
c-Src
Y416P-c-Src
HA-S1P2
Lamin
S1P - + - + - + - +
RB-005 - - + + - - + +
Vector
HA-S1P2

Fig. 2B

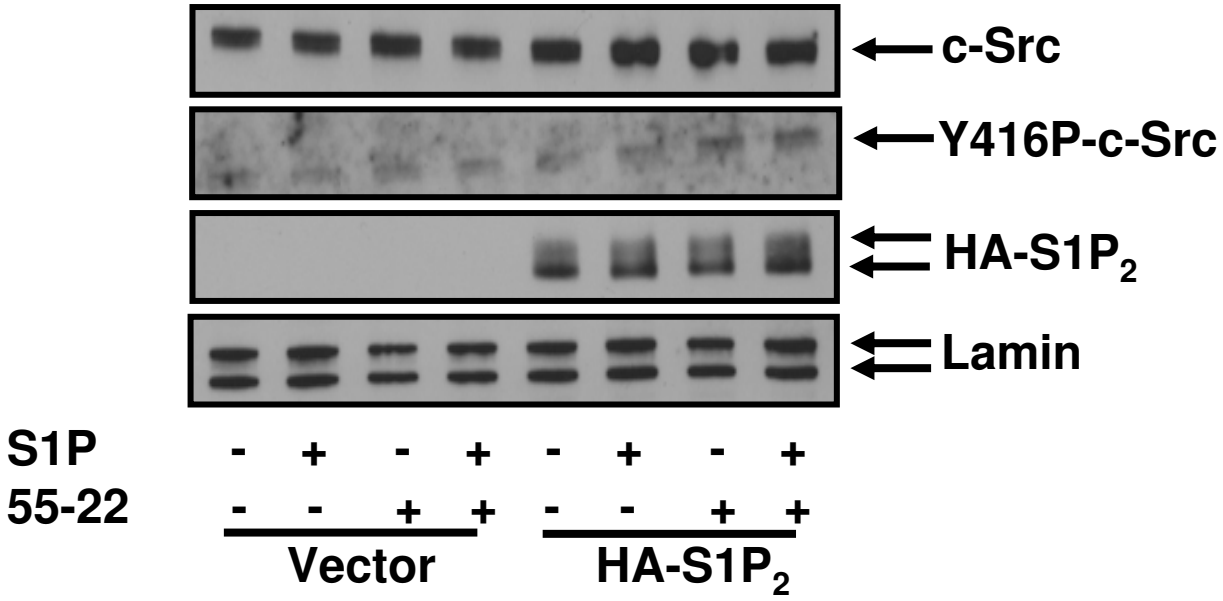
c-Src
Y416P-c-Src
HA-S1P2
Lamin
S1P - + - + - + - +
55-22 - - + + - - + +
Vector
HA-S1P2

Fig. 2C

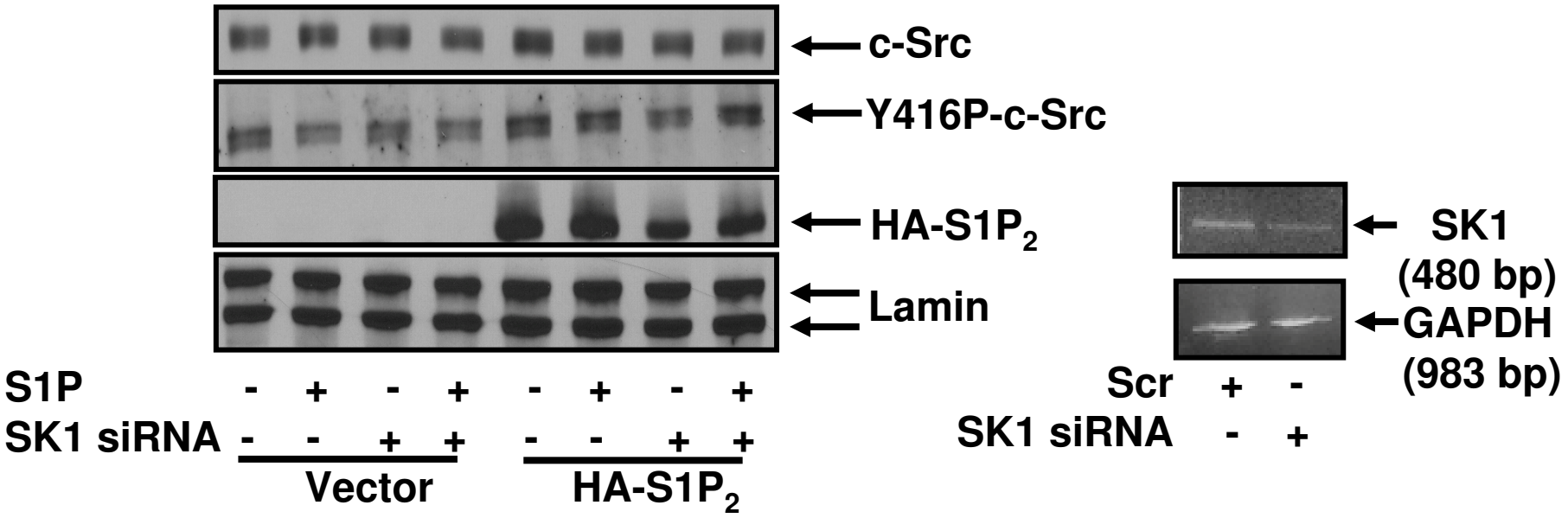
c-Src
Y416P-c-Src
HA-S1P2
Lamin
S1P - + - + - + - +
SK1 siRNA - - + + - - + +
Vector
HA-S1P2
SK1
(480 bp)
GAPDH
(983 bp)
Scr + -
SK1 siRNA - +

Fig. 2D

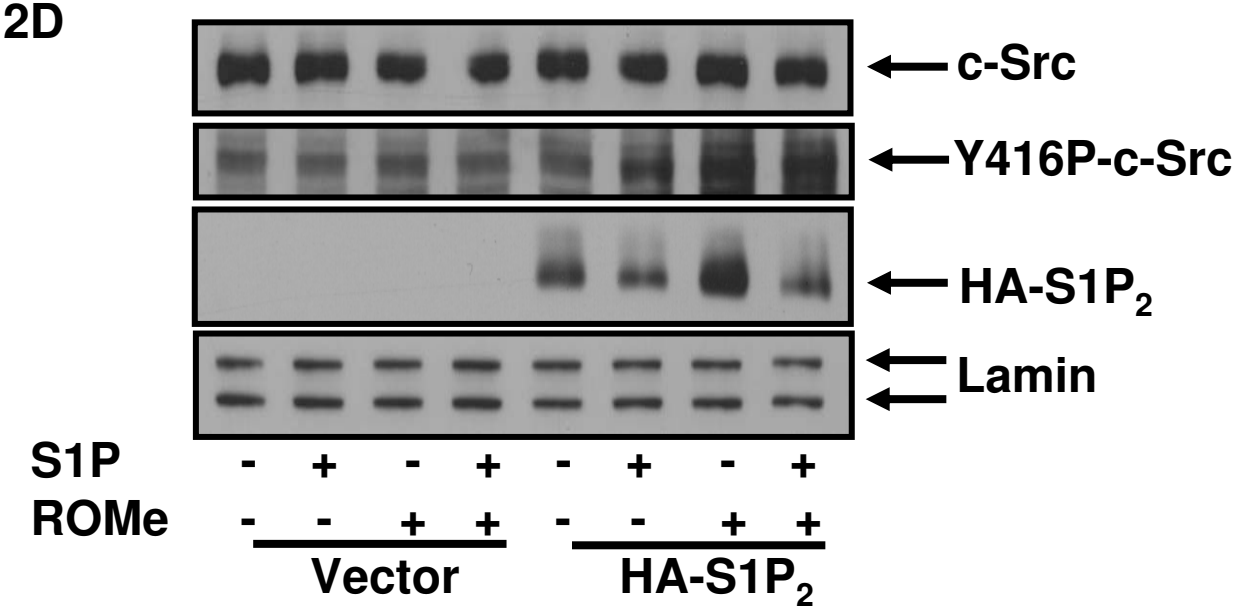
c-Src
Y416P-c-Src
HA-S1P2
Lamin
S1P - + - + - + - +
ROMe - - + + - - + +
Vector
HA-S1P2

Fig. 2E

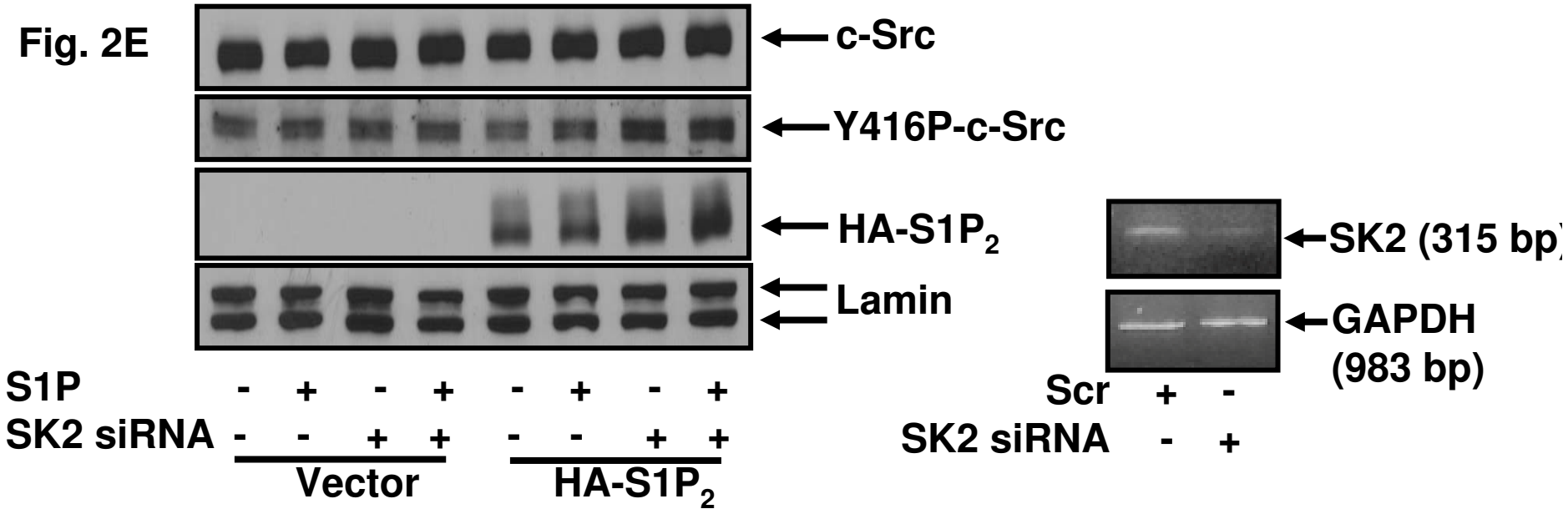
c-Src
Y416P-c-Src
HA-S1P2
Lamin
S1P - + - + - + - +
SK2 siRNA - - + + - - + +
Vector
HA-S1P2
SK2 (315 bp)
GAPDH
(983 bp)
Scr + -
SK2 siRNA - +

Fig. 2F

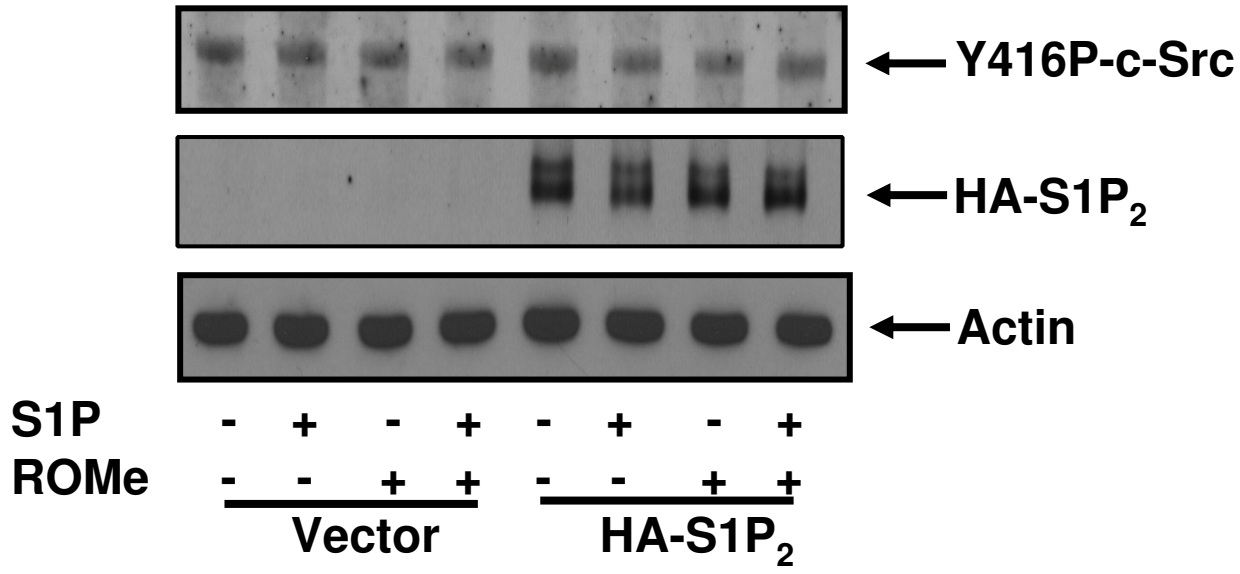

Fig. 3A

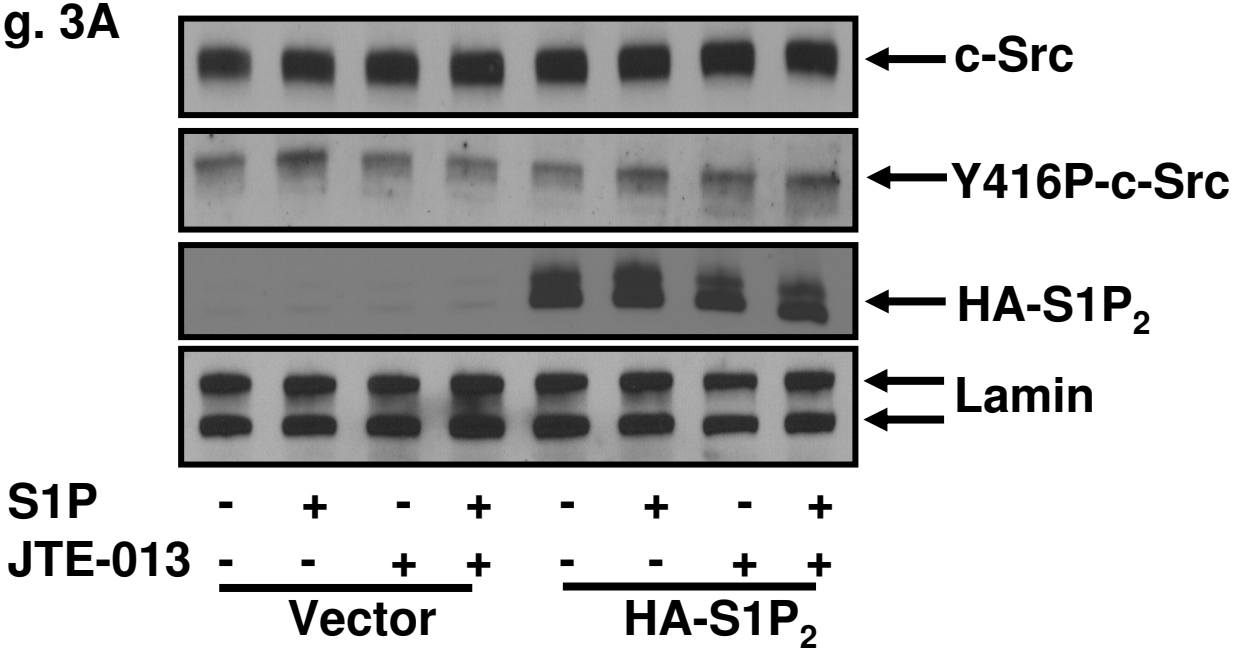
c-Src
Y416P-c-Src
HA-S1P2
Lamin
S1P - + - + - + - +
JTE-013 - - + + - - + +
Vector
HA-S1P2

Fig. 3B

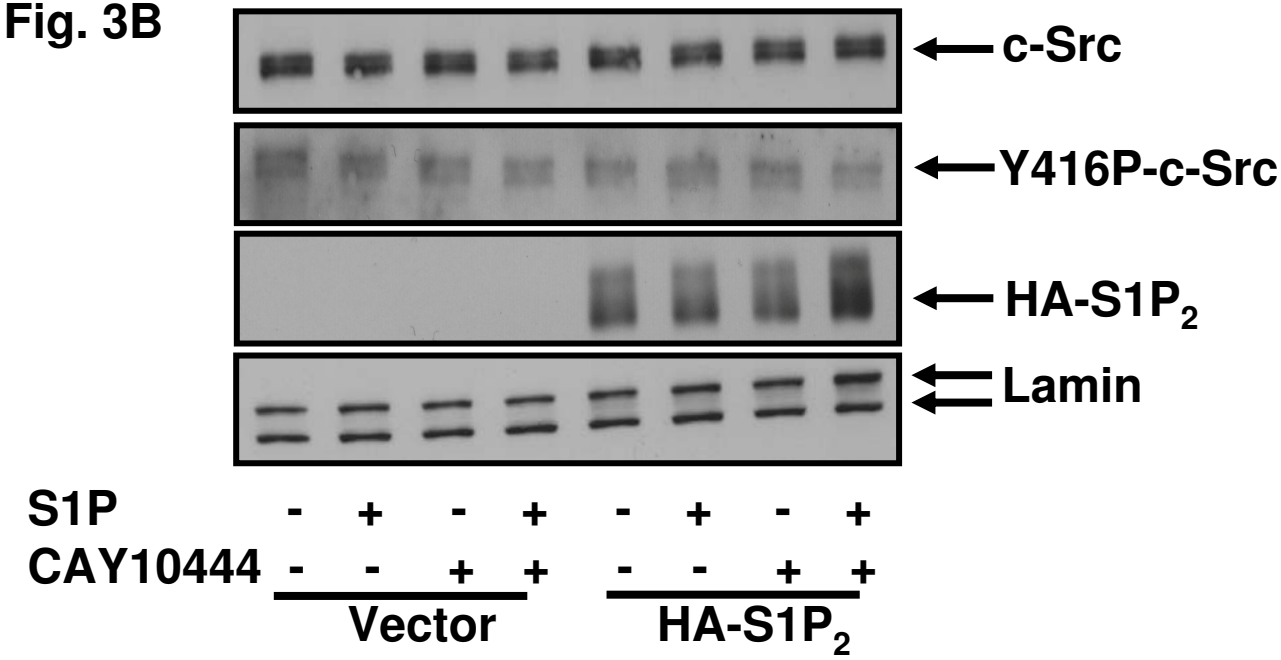
c-Src
Y416P-c-Src
HA-S1P2
Lamin
S1P - + - + - + - +
CAY10444 - - + + - - + +
Vector
HA-S1P2

Fig. 3C

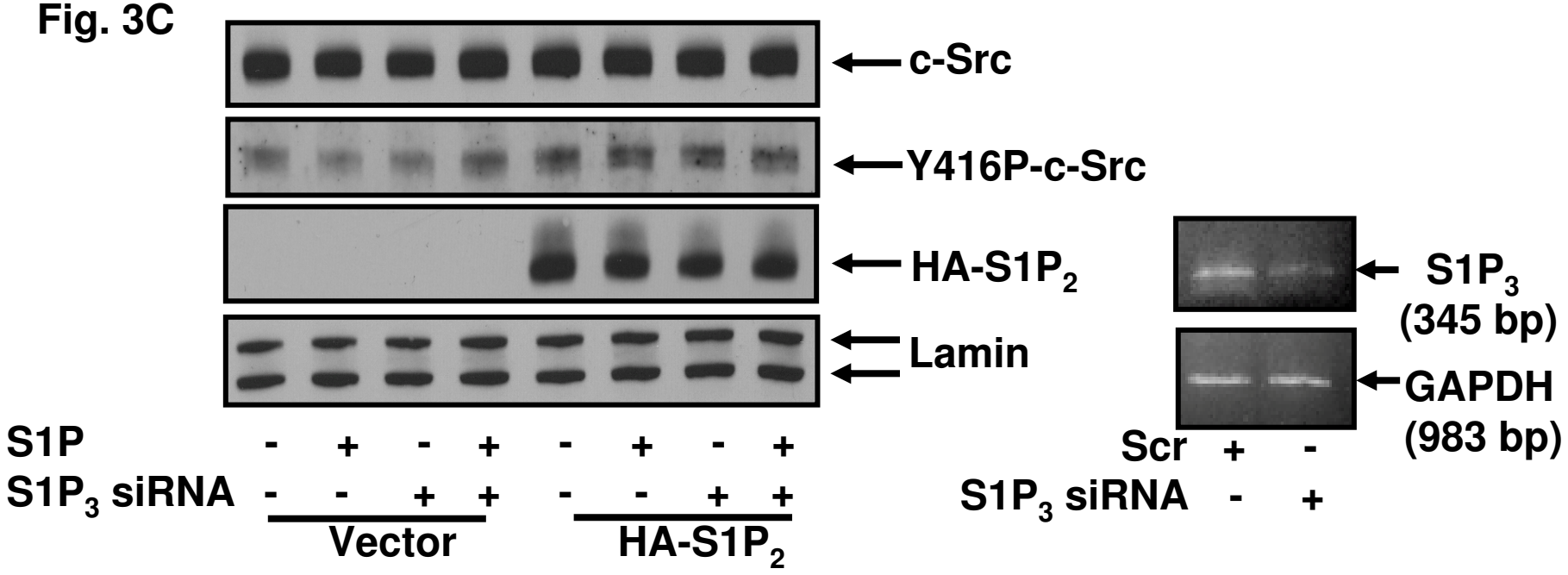
c-Src
Y416P-c-Src
HA-S1P2
Lamin
S1P
S1P3 siRNA
Vector
HA-S1P2
S1P3
(345 bp)
GAPDH
(983 bp)
Scr
S1P3 siRNA

Fig. 3D

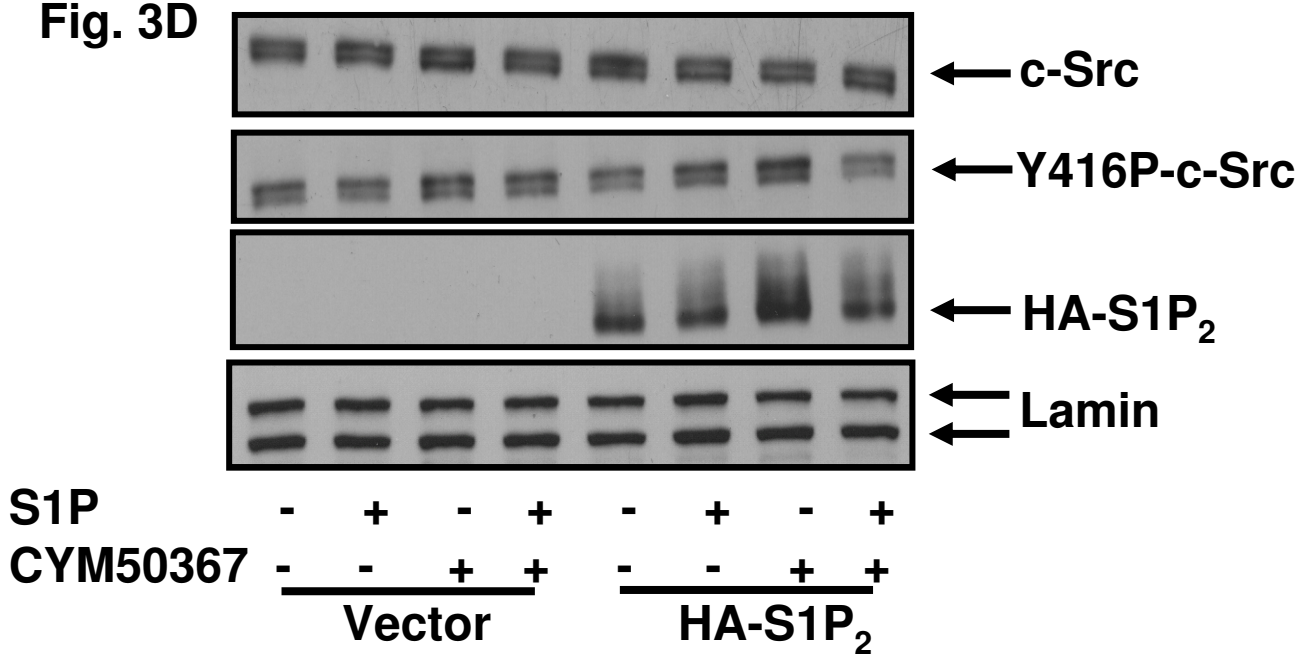
c-Src
Y416P-c-Src
HA-S1P2
Lamin
S1P - + - + - + - +
CYM50367 - - + + - - + +
Vector
HA-S1P2

Fig. 3E

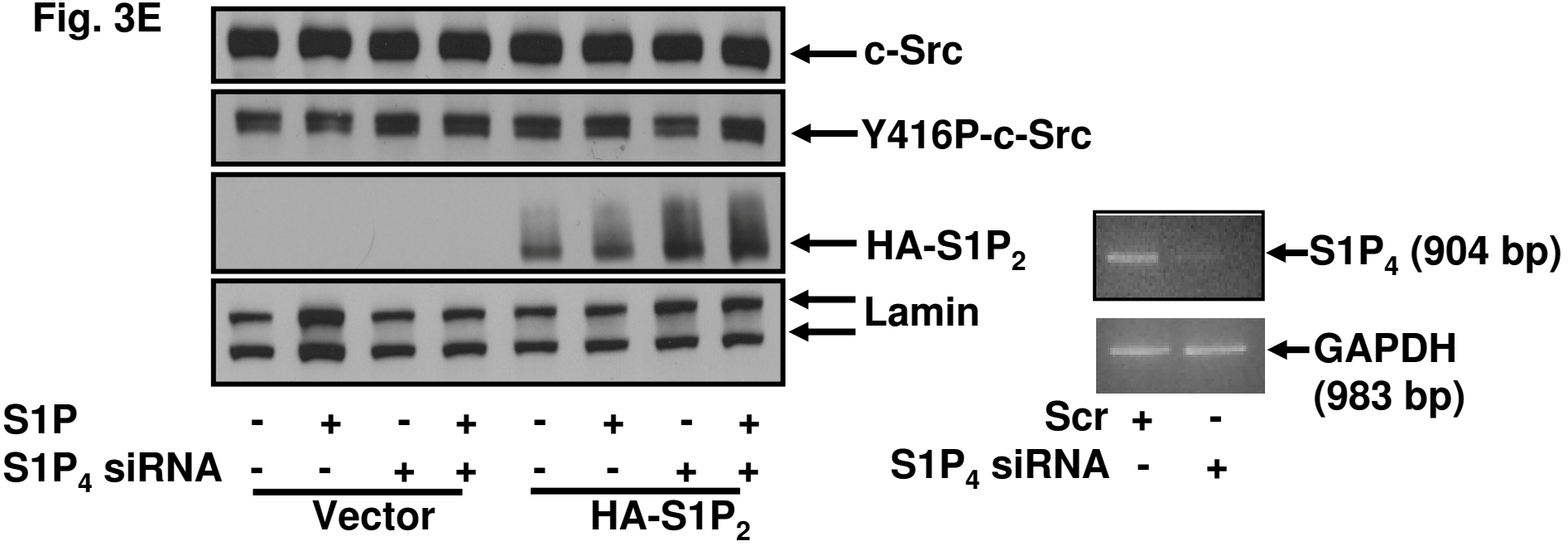
c-Src
Y416P-c-Src
HA-S1P2
Lamin
S1P4 (904 bp)
GAPDH
(983 bp)
S1P - + - + - + - +
S1P4 siRNA - - + + - - + +
Vector
HA-S1P2
Scr + -
S1P4 siRNA - +

Fig. 3F

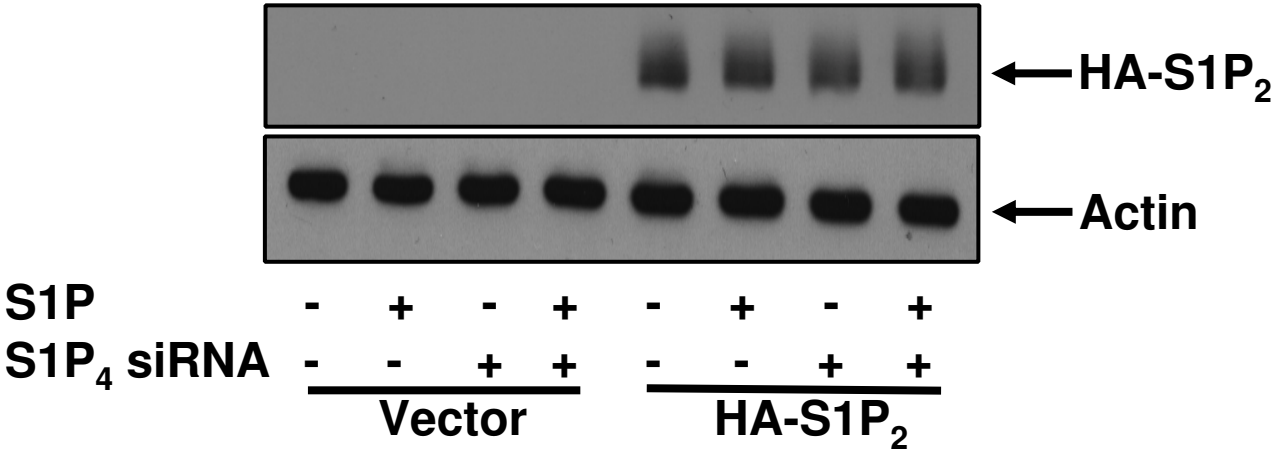

Fig. 4

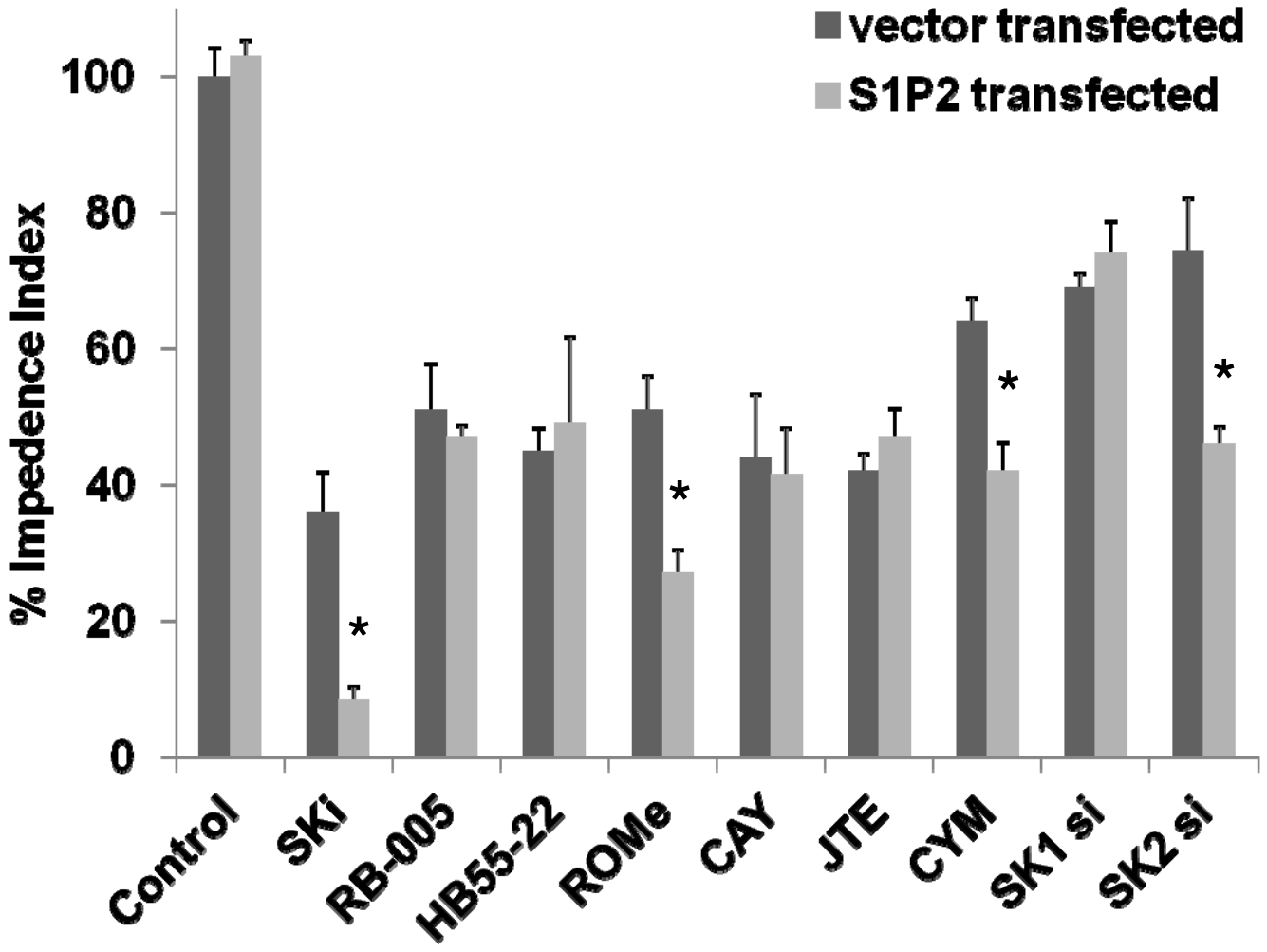
vector transfected
S1P2 transfected
% Impedence Index
100
80
60
40
20
0
*
*
*
Control
SKi
RB-005
HB55-22
ROMe
CAY
JTE
CYM
SK1 si
SK2 si

Fig. 5A

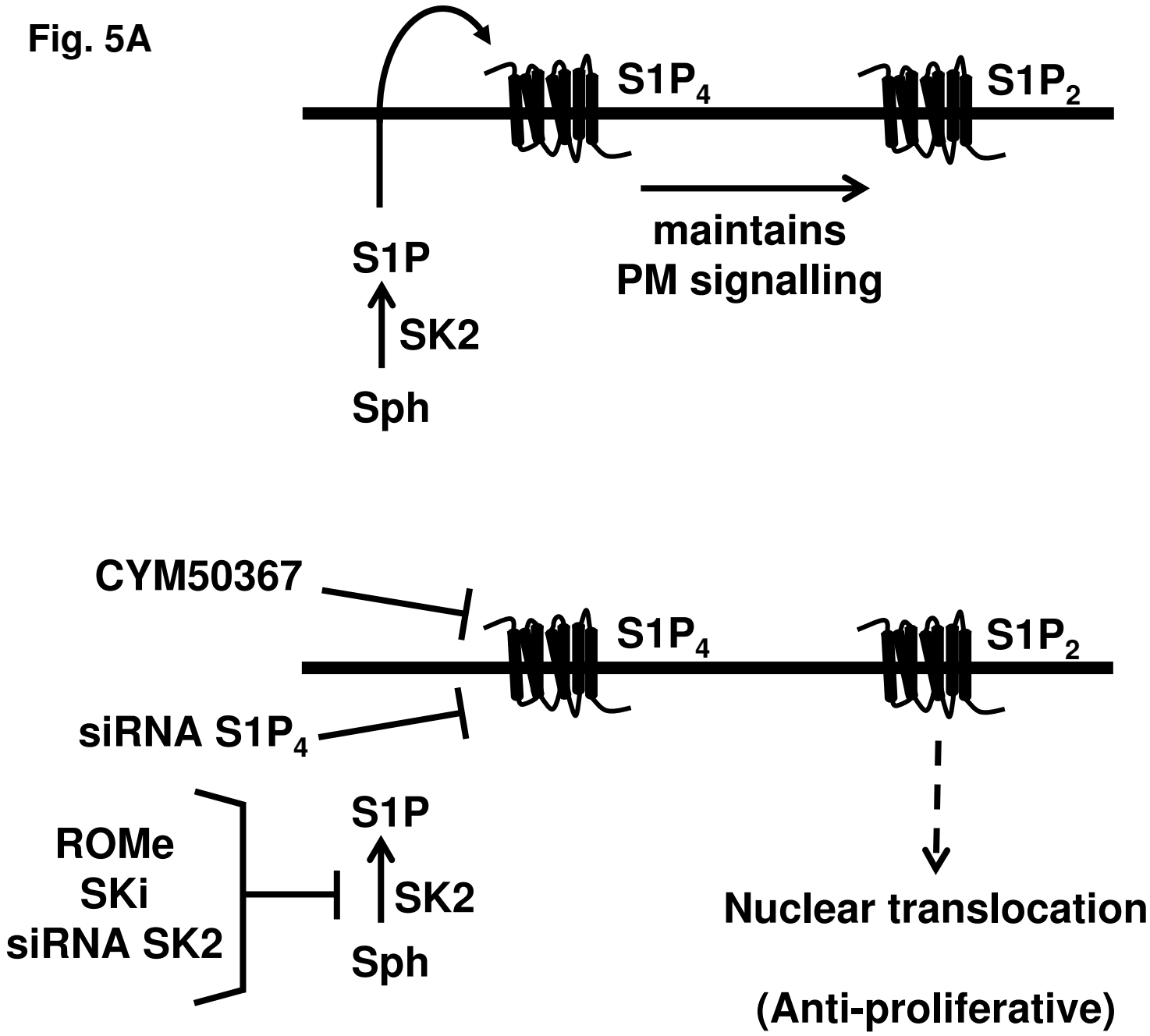
S1P4
S1P2
maintains
PM signalling
S1P
SK2
Sph
CYM50367
S1P4
S1P2
siRNA S1P4
ROMe
SKi
siRNA SK2
S1P
SK2
Sph
Nuclear translocation
(Anti-proliferative)

Fig. 5B

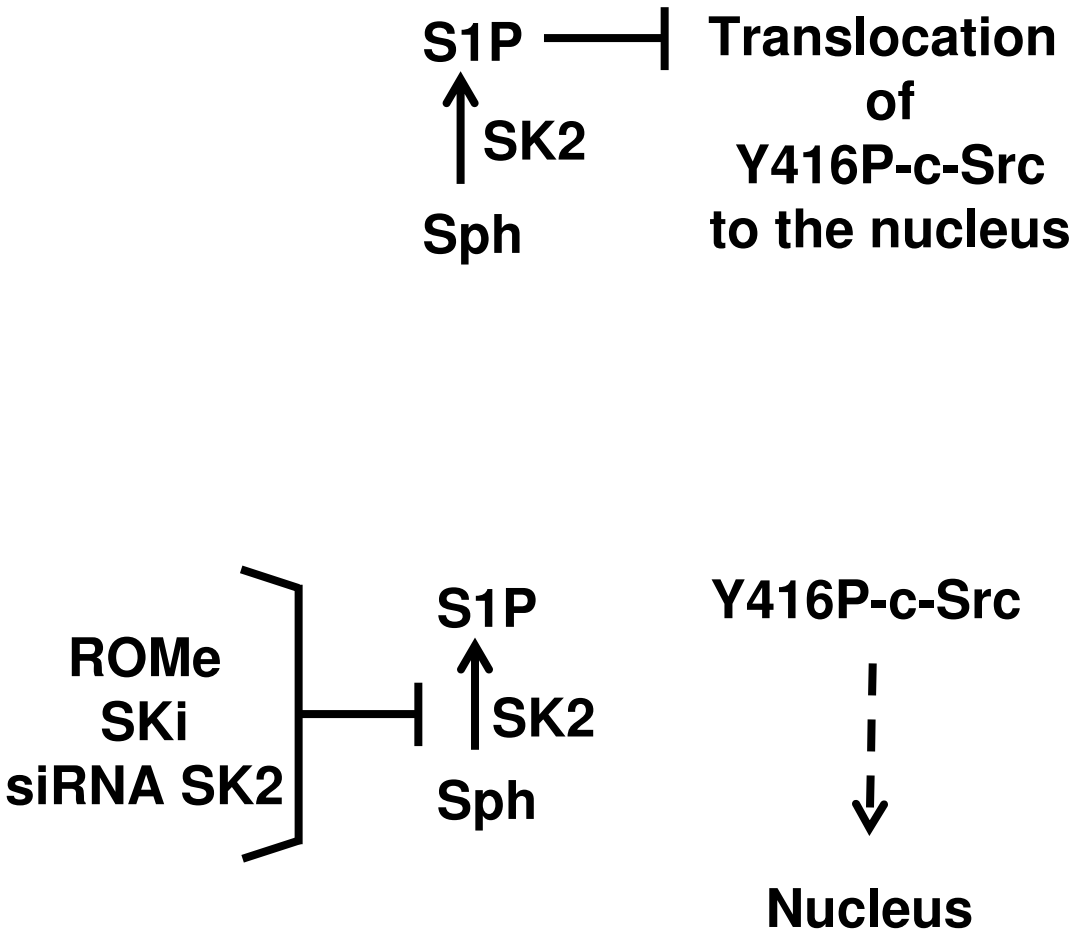
S1P
SK2
Sph
Translocation
of
Y416P-c-Src
to the nucleus
ROMe
SKi
siRNA SK2
S1P
SK2
Sph
Y416P-c-Src
Nucleus

Supplemental Figure legends

Suppl Figure 1. Quantification of the effect of SKi on the nuclear localization of HA-tagged $S1P_2$, c-Src and Y416 phosphorylated Src (pSrc) in HA-$S1P_2$-transfected MDA-MB-231 cells. Nuclear HA-$S1P_2$, c-Src and pSrc were quantified relative to nuclear lamin levels. Control levels are set at 100 +/- SEM % and results are from n=3 experiments.

Suppl Figure 2. Quantification of the effect of SKi on Y416 phosphorylated Src (pSrc) levels in cell lysates from vector- and HA-$S1P_2$- transfected MDA-MB-231 cells. pSrc was quantified relative to actin levels. Control levels are set at 100 +/- SEM % and results are from n=3 experiments.

Suppl Figure 3. Quantification of the effect of SKi on nuclear Y416 phosphorylated Src (pSrc) and c-Src levels in vector-transfected MDA-MB-231 cells. Nuclear c-Src and pSrc were quantified relative to lamin levels. Control levels are set at 100 +/- SEM % and results are from n=3 experiments.

Suppl Figure 4. Quantification of the effect of SKi on nuclear HA-tagged $S1P_2$ and Y416 phosphorylated Src (pSrc) levels in HA-$S1P_2$- transfected MCF-7 cells. Nuclear HA-tagged $S1P_2$ and pSrc were quantified relative to lamin levels. Control levels are set at 100 +/- SEM % and results are from n=3 experiments.

Suppl Figure 5. Quantification of the effect of (A) RB-005; (B) 55-22; (C) SK1 siRNA; (D) ROMe; (E) SK2 siRNA on the nuclear localization of HA-tagged $S1P_2$ and Y416 phosphorylated Src (pSrc) in HA-$S1P_2$-transfected MDA-MB-231 cells. Nuclear HA-$S1P_2$ and pSrc were quantified relative to nuclear lamin levels. Control levels are set at 100 +/- SEM % and results are from n=3 experiments.

Suppl Figure 6. Quantification of the effect of ROMe on Y416 phosphorylated Src (pSrc) levels in cell lysates from vector- and HA-$S1P_2$- transfected MDA-MB-231 cells. pSrc was quantified relative to actin levels. Control levels are set at 100 +/- SEM % and results are from n=3 experiments.

Suppl Figure 7. Quantification of the effect of (A) JTE-013; (B) CAY10444; (C) $S1P_3$ siRNA; (D) CYM50637; (E) $S1P_4$ siRNA on the nuclear localization of HA-tagged $S1P_2$ and Y416 phosphorylated Src (pSrc) in HA-$S1P_2$-transfected MDA-MB-231 cells. Nuclear HA-$S1P_2$ and pSrc were quantified relative to nuclear lamin levels. Control levels are set at 100 +/- SEM % and results are from n=3 experiments.

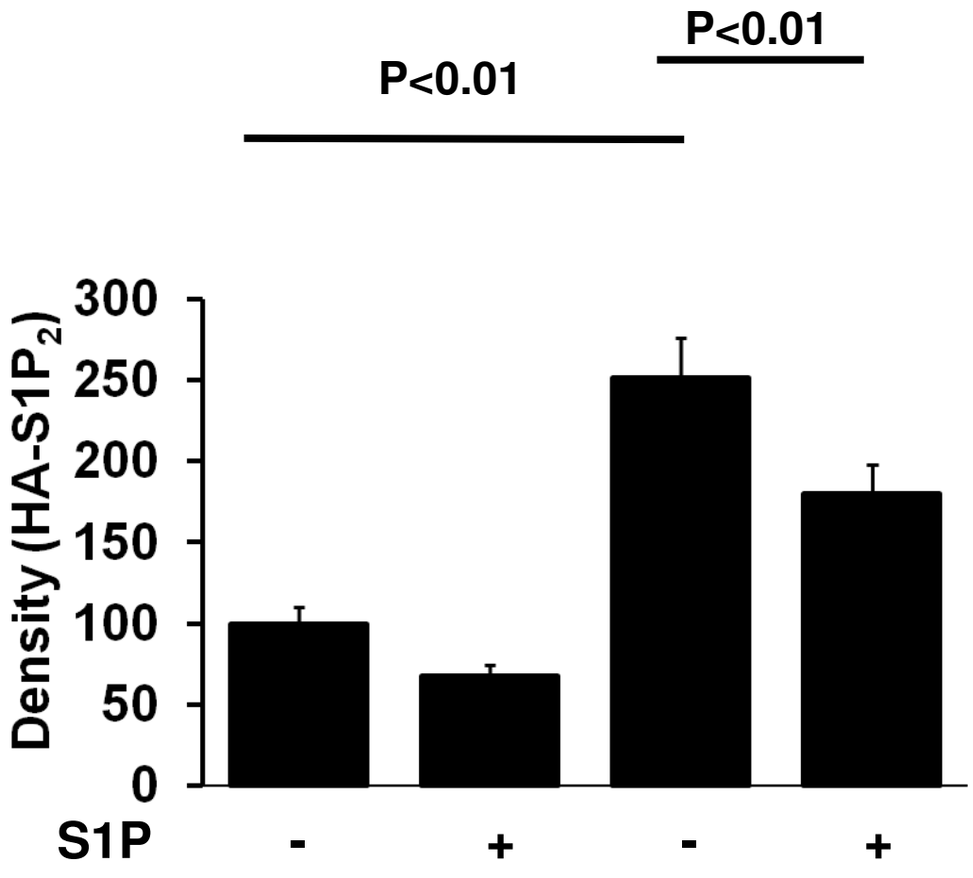
P<0.01
P<0.01
Density (HA-S1P2)
300
250
200
150
100
50
0
S1P
-
+
-
+
SKi
-
-
+
+

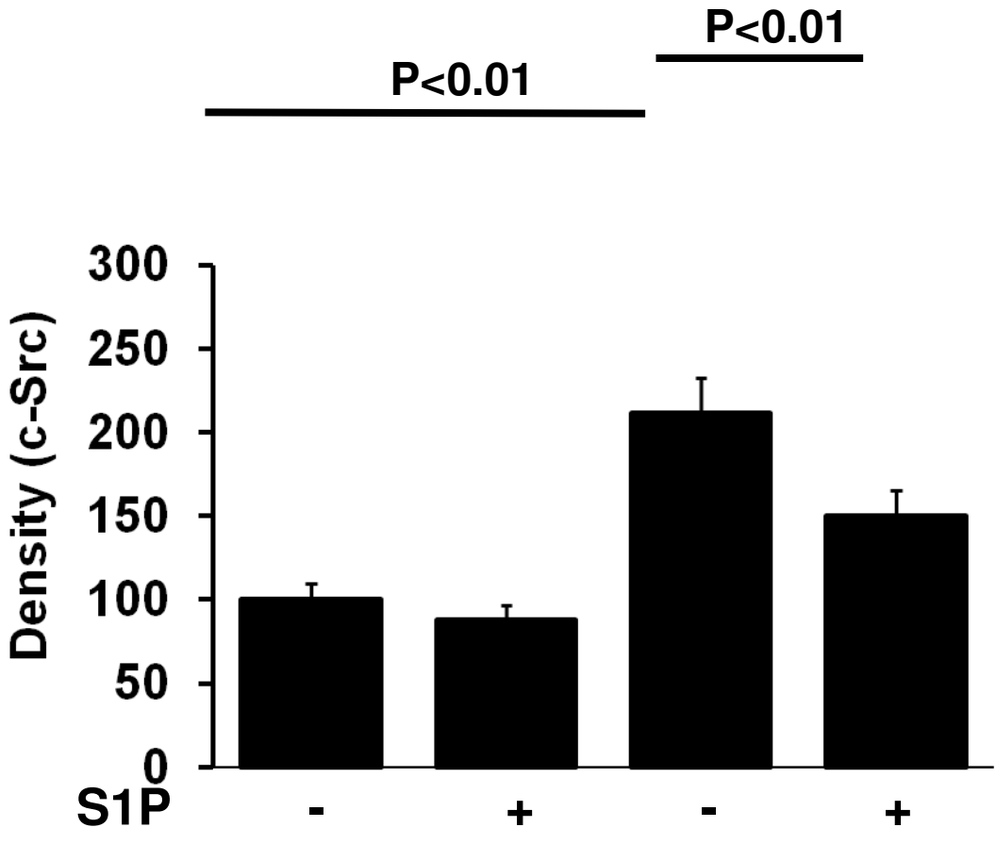
P<0.01
P<0.01
Density (c-Src)
300
250
200
150
100
50
0
S1P
-
+
-
+
SKi
-
-
+
+

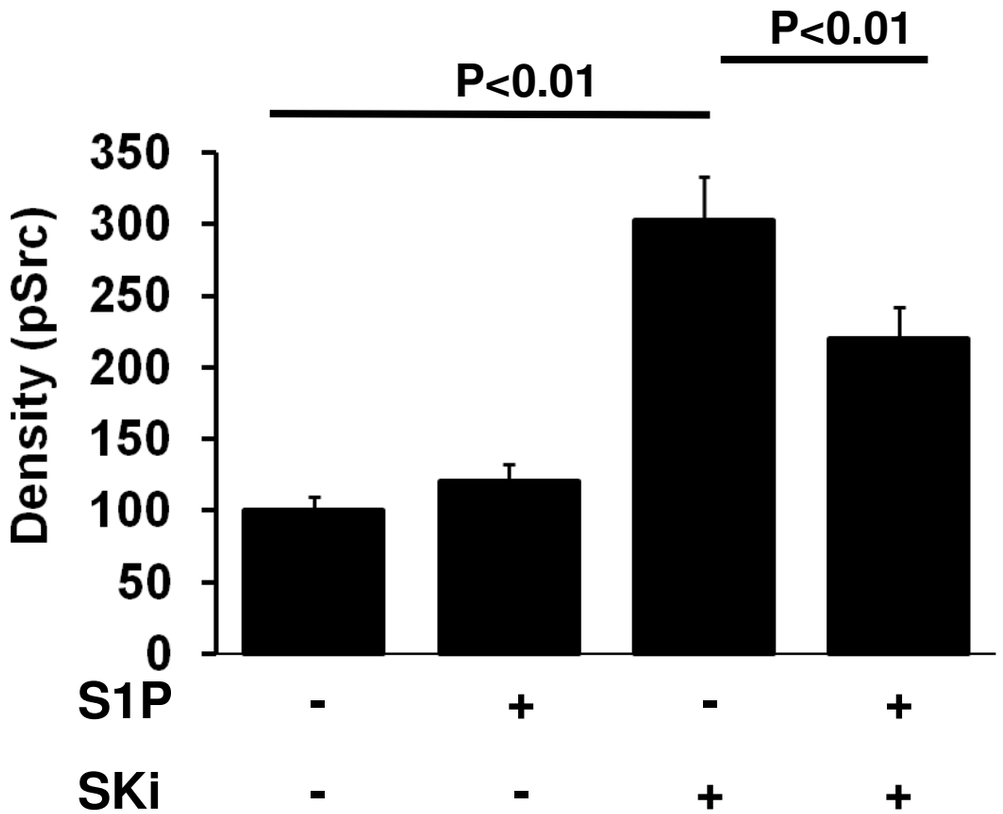
P<0.01
P<0.01
Density (pSrc)
350
300
250
200
150
100
50
0
S1P
-
+
-
+
SKi
-
-
+
+

Suppl. Fig. 1

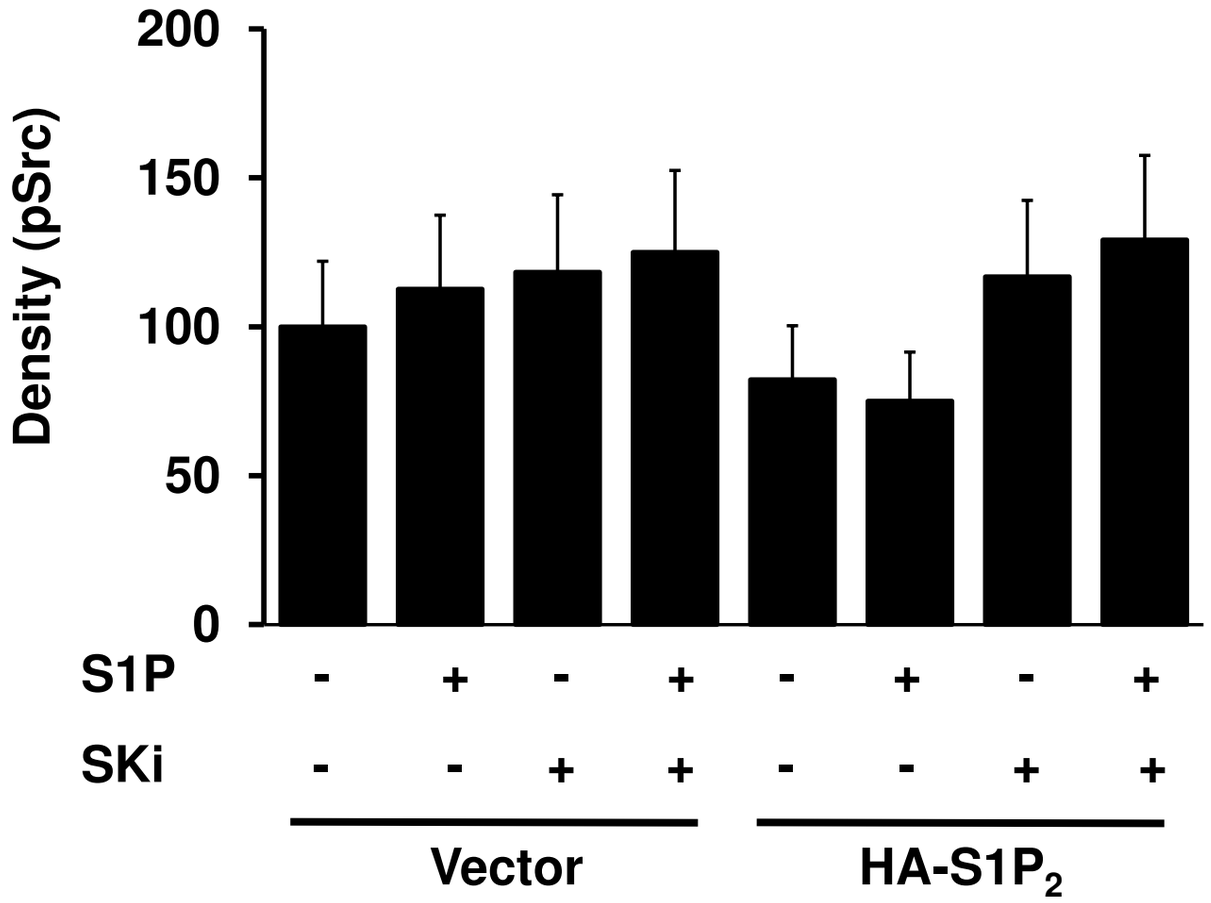

Suppl.
Fig. 2

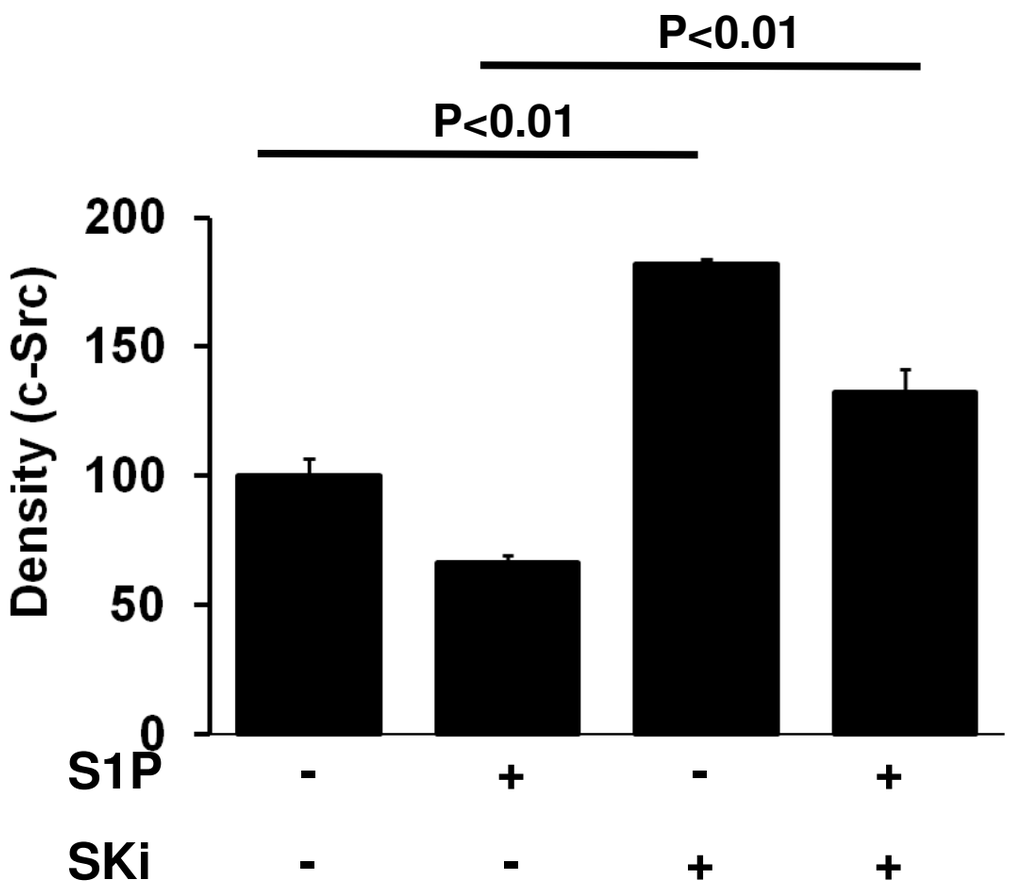
P<0.01
P<0.01
Density (c-Src)
200
150
100
50
0
S1P
SKi
-
+
-
+
-
-
+
+

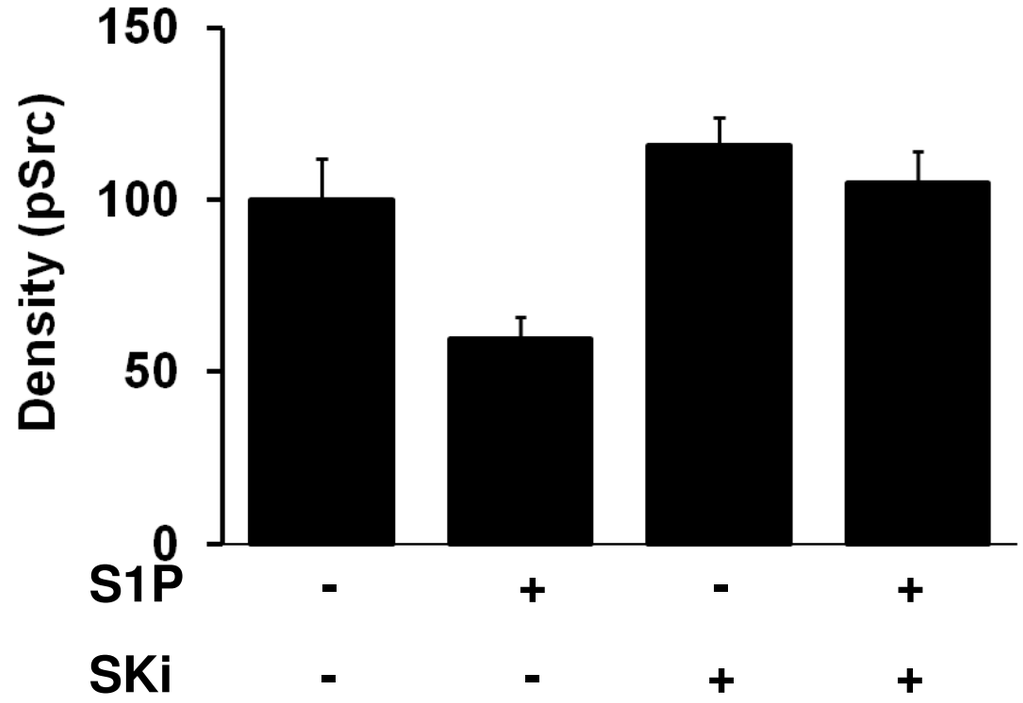
Density (pSrc)
150
100
50
0
S1P
SKi
-
+
-
+
-
-
+
+

Suppl.
Fig. 3

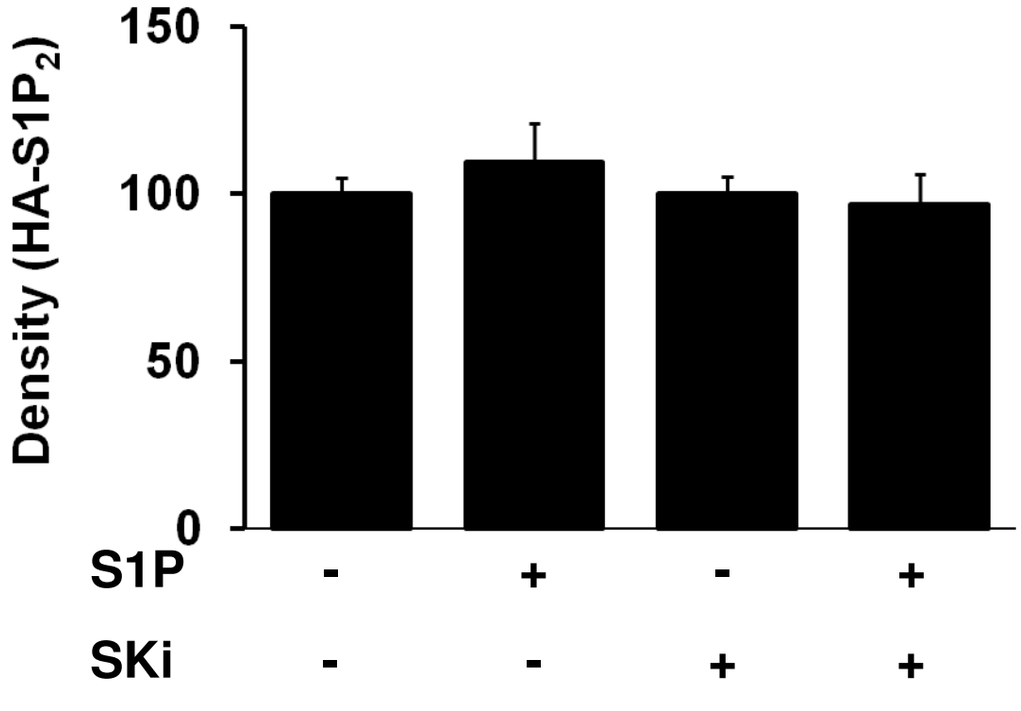
Density (HA-S1P2)
150
100
50
0
S1P - + - +
SKi - - + +

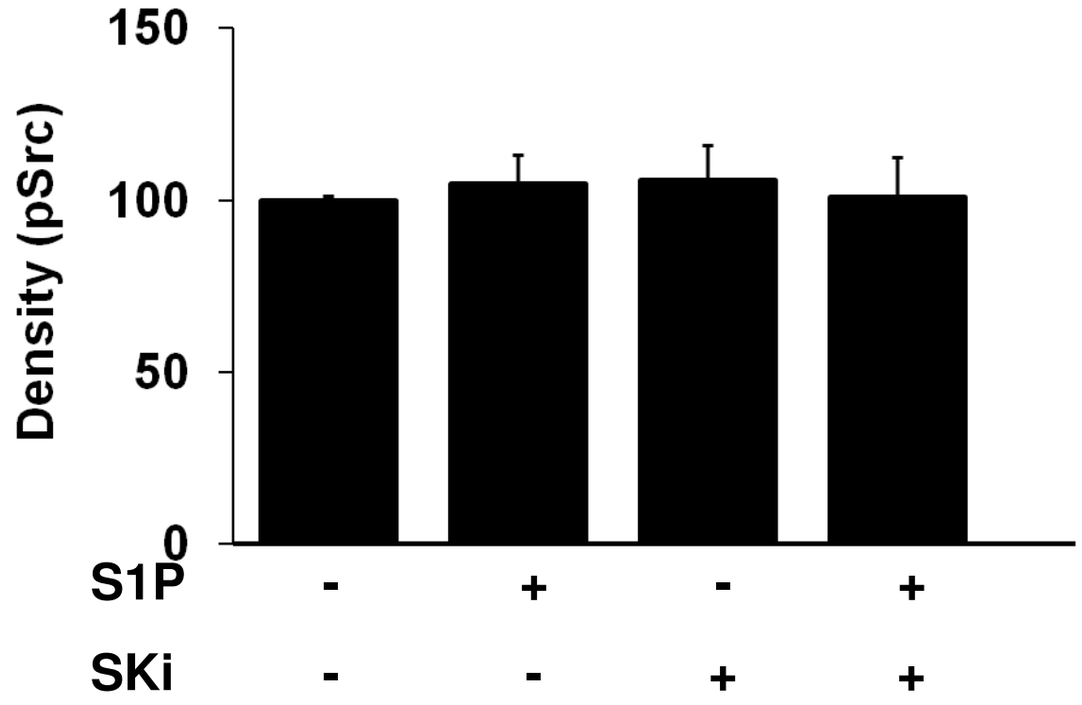
Density (pSrc)
150
100
50
0
S1P - + - +
SKi - - + +

Suppl.
Fig. 4

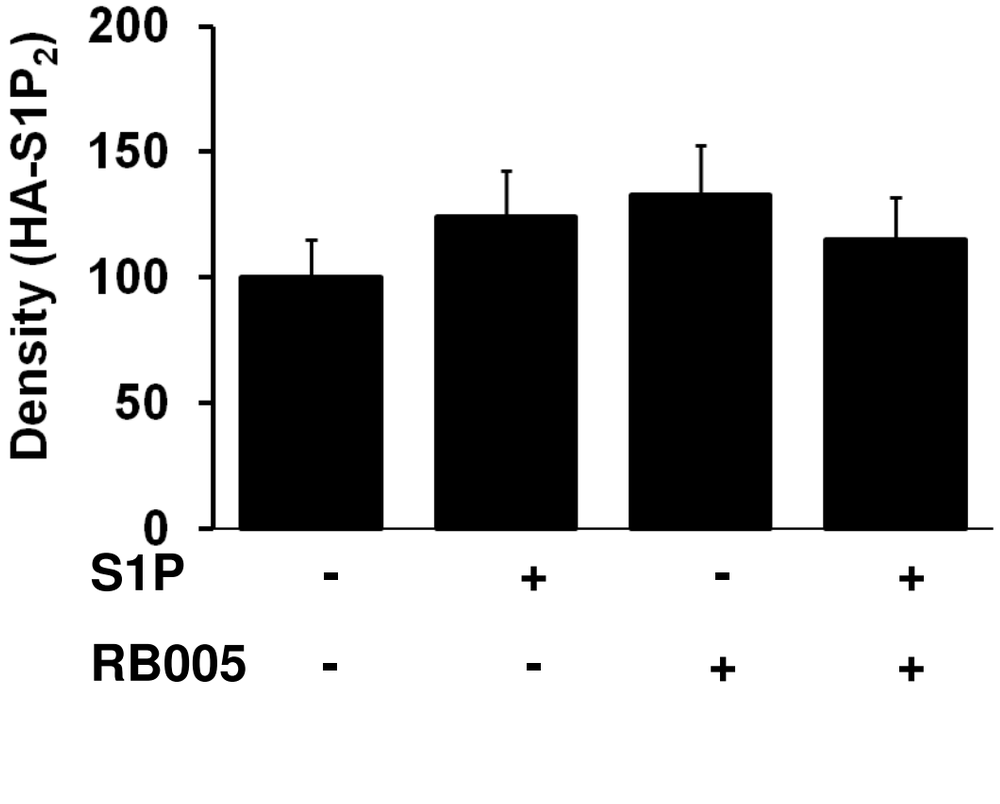
Density (HA-S1P2)
200
150
100
50
0
S1P - + - +
RB005 - - + +

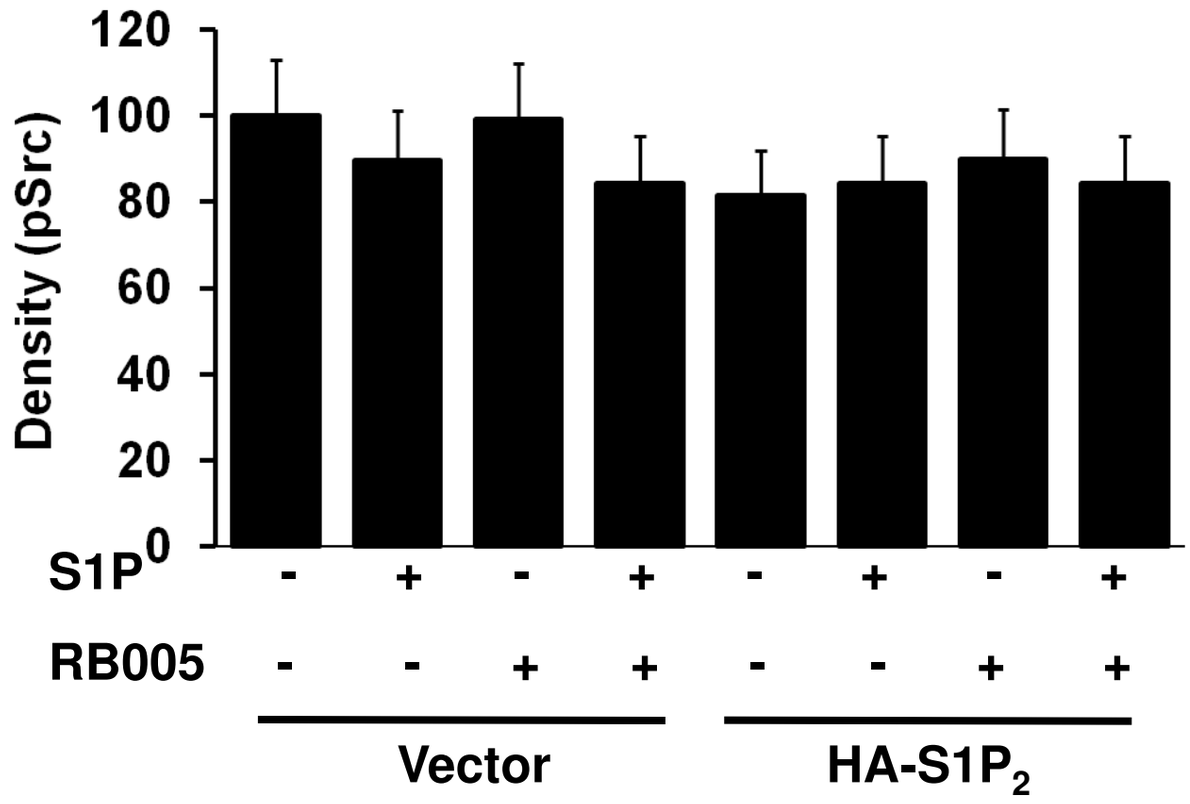
Density (pSrc)
120
100
80
60
40
20
0
S1P - + - + - + - +
RB005 - - + + - - + +
Vector
HA-S1P2

Suppl.
Fig. 5A

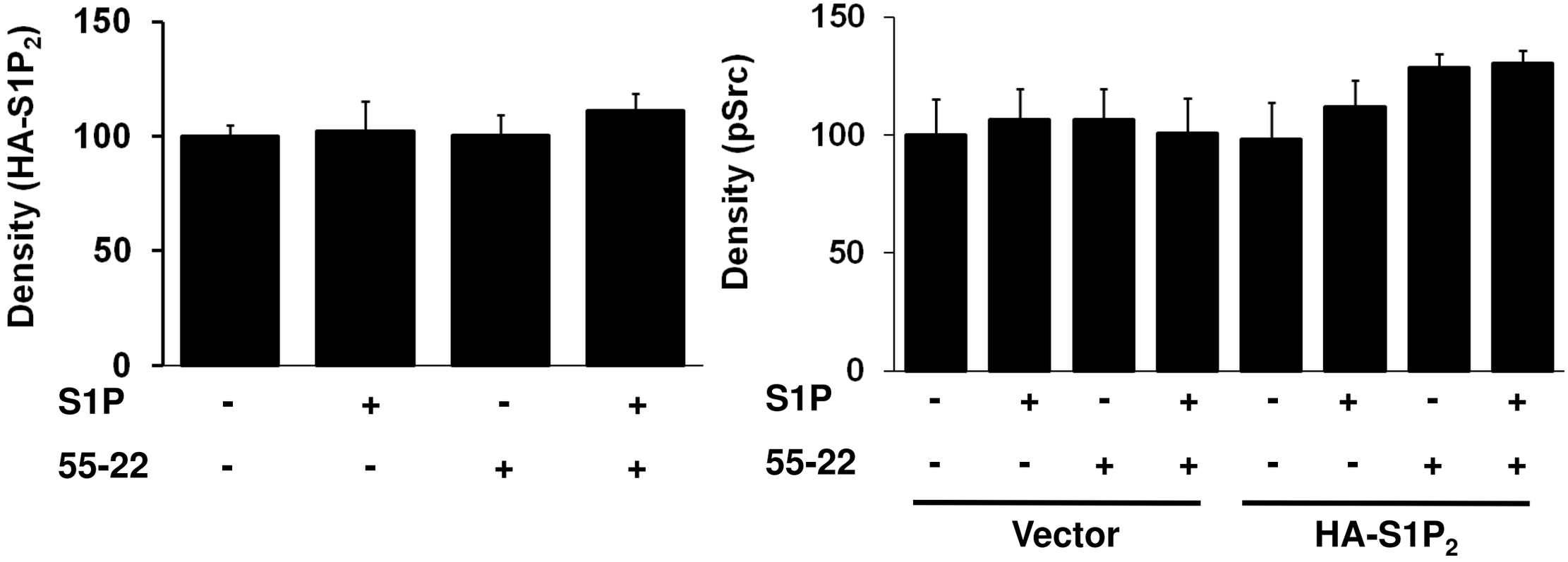
Density (HA-S1P2)
150
100
50
0
S1P - + - +
55-22 - - + +
Density (pSrc)
150
100
50
0
S1P - + - + - + - +
55-22 - - + + - - + +
Vector
HA-S1P2

Suppl.
Fig. 5B

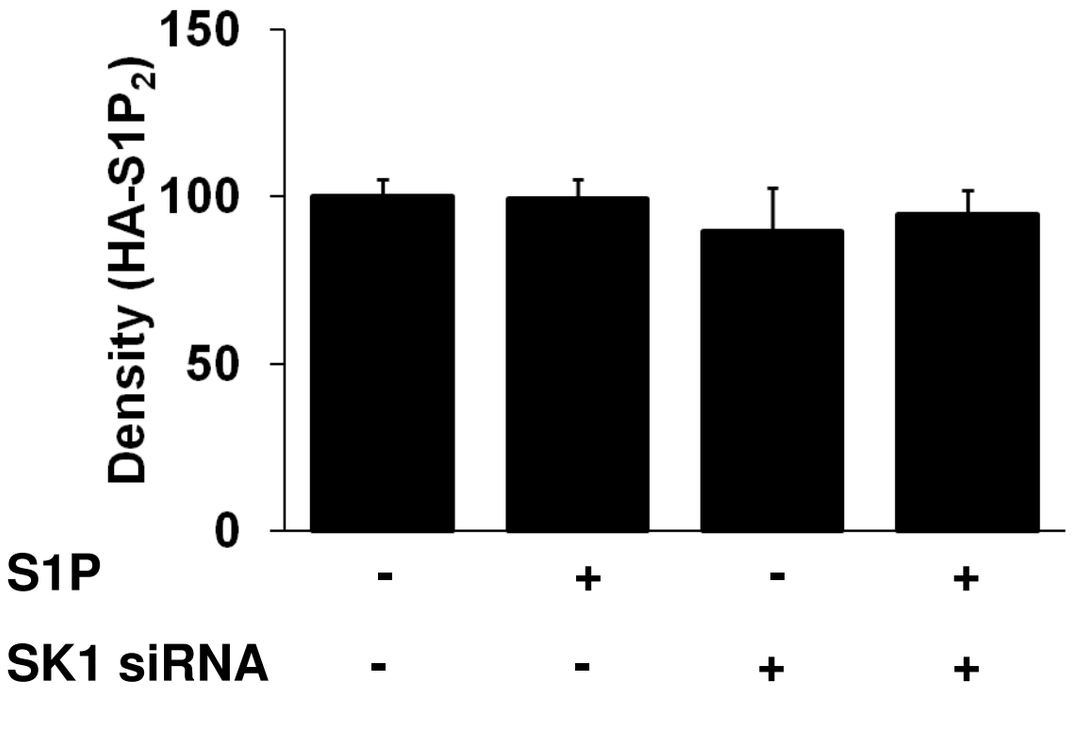
Density (HA-S1P2)
150
100
50
0
S1P
-
+
-
+
SK1 siRNA
-
-
+
+

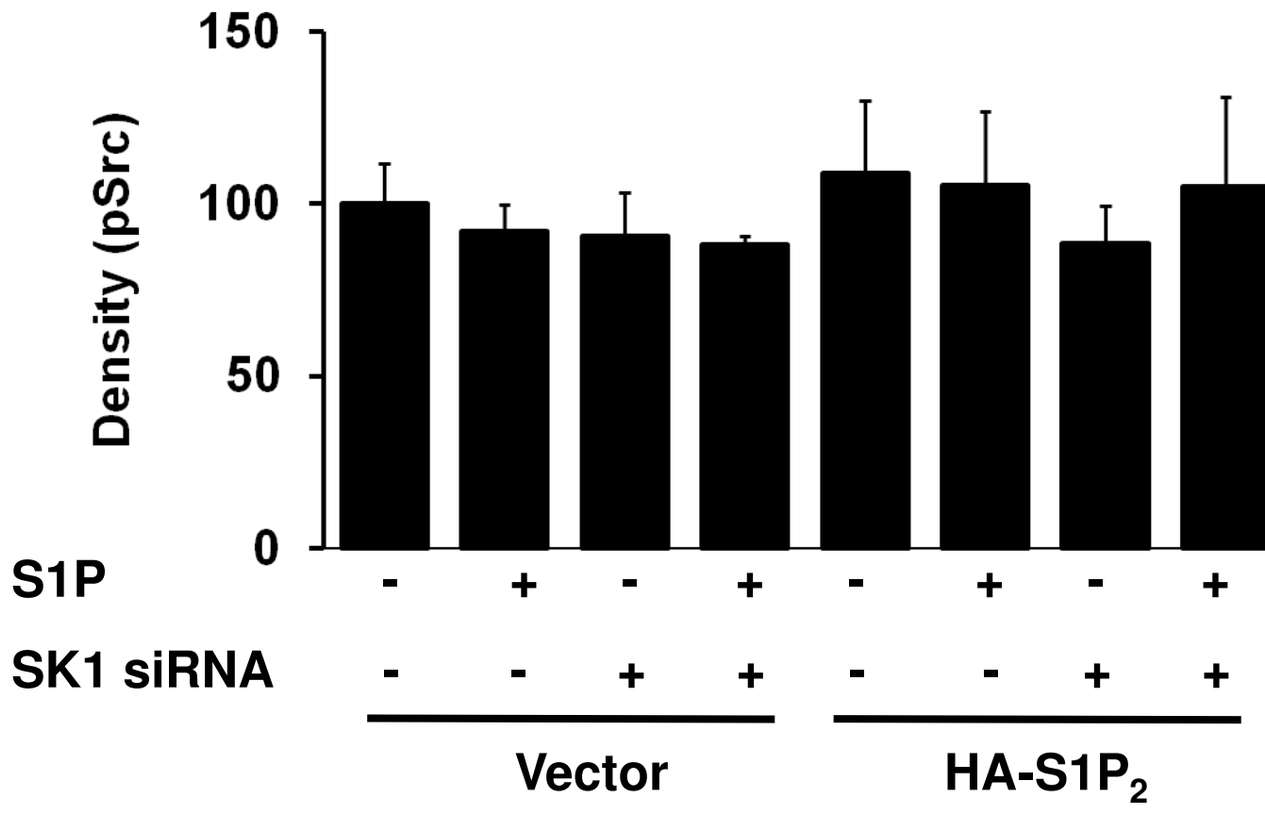
Density (pSrc)
150
100
50
0
S1P
-
+
-
+
-
+
-
+
SK1 siRNA
-
-
+
+
-
-
+
+
Vector
HA-S1P2

Suppl.
Fig. 5C

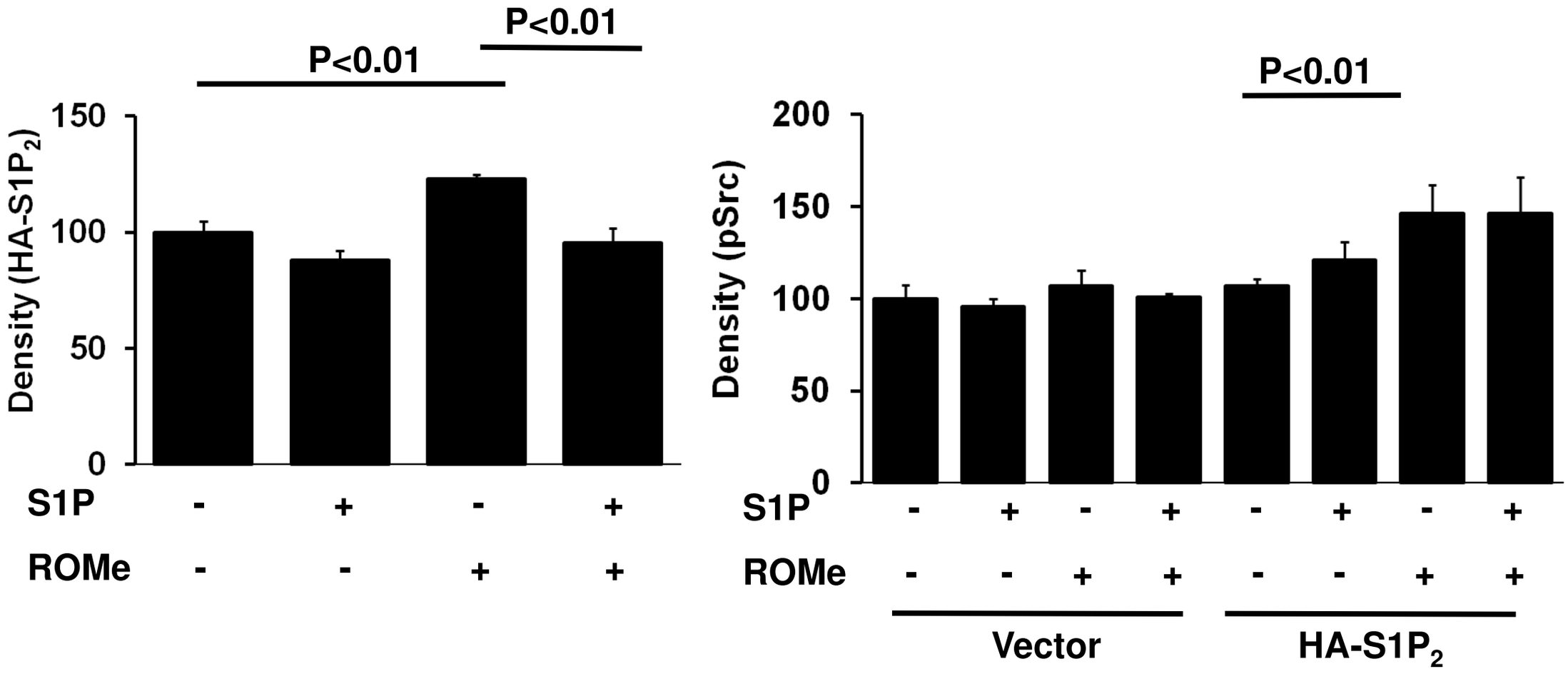
P<0.01
P<0.01
Density (HA-S1P2)
150
100
50
0
S1P - + - +
ROMe - - + +
P<0.01
Density (pSrc)
200
150
100
50
0
S1P - + - + - + - +
ROMe - - + + - - + +
Vector
HA-S1P2

Suppl.
Fig. 5D

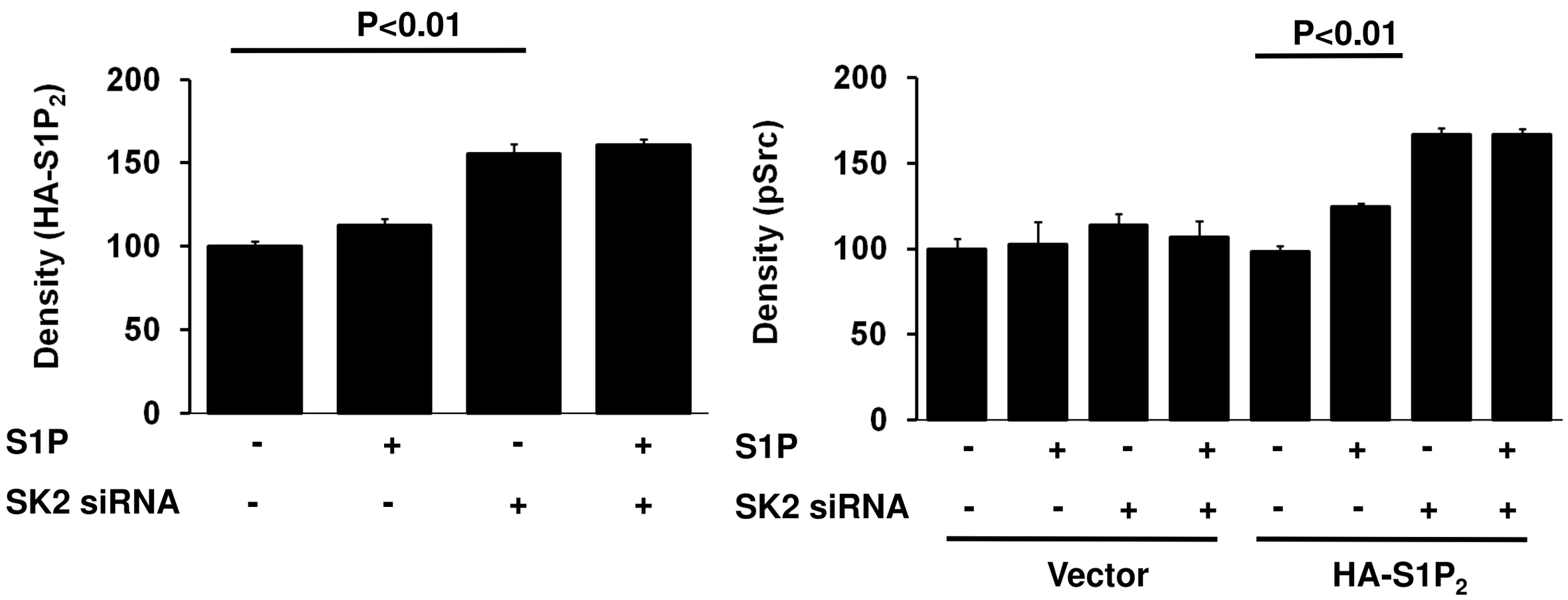
P<0.01
Density (HA-S1P2)
200
150
100
50
0
S1P
-
+
-
+
SK2 siRNA
-
-
+
+
P<0.01
Density (pSrc)
200
150
100
50
0
S1P
-
+
-
+
-
+
-
+
SK2 siRNA
-
-
+
+
-
-
+
+
Vector
HA-S1P2

Suppl.
Fig. 5E

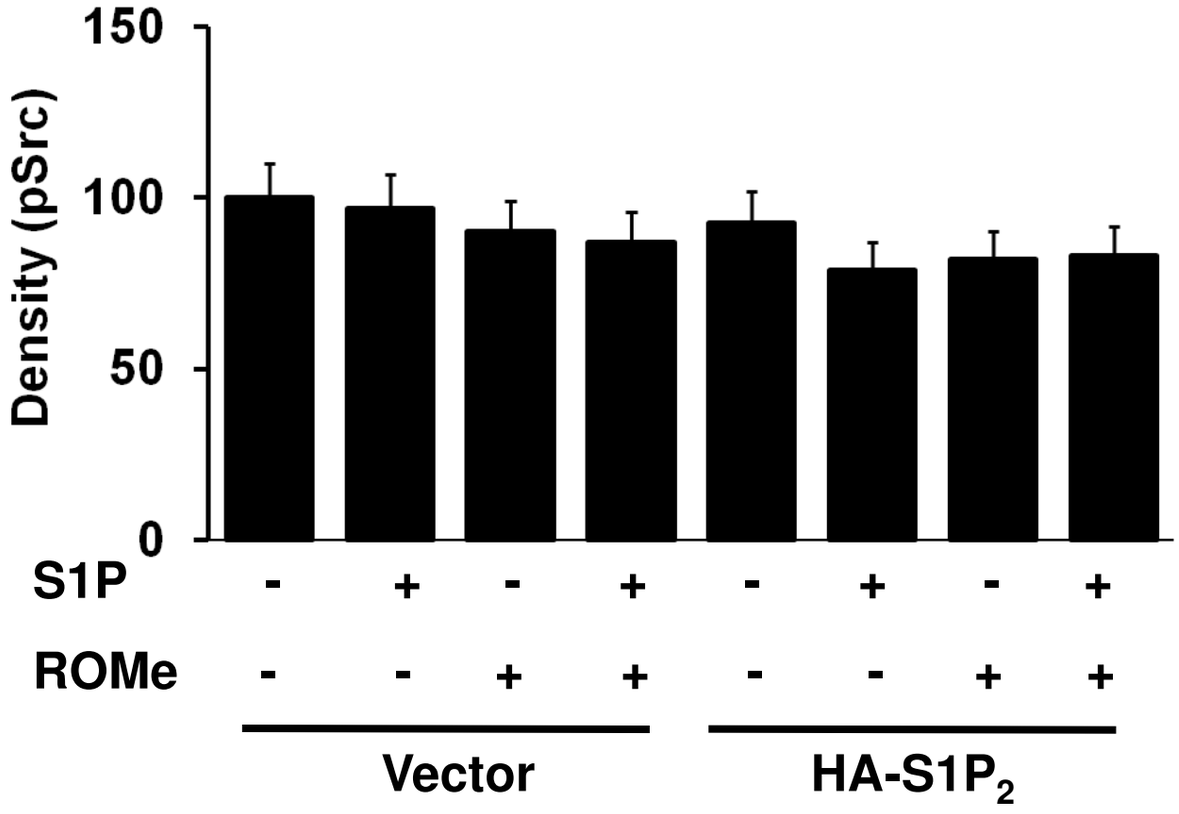

Suppl.
Fig. 6

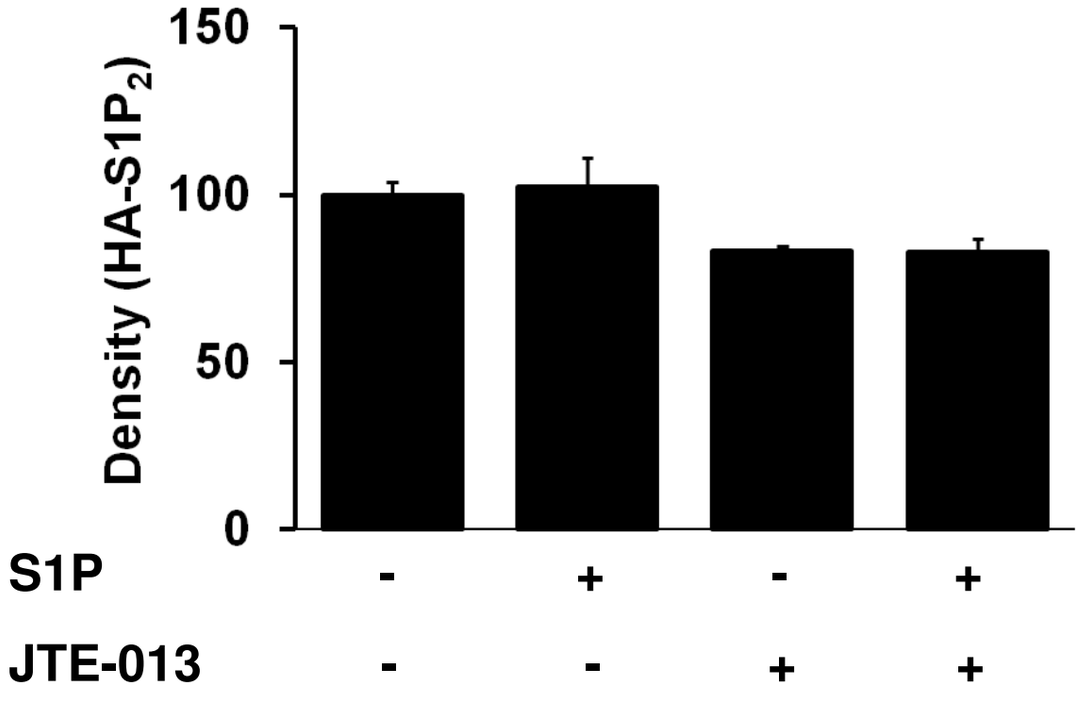
Density (HA-S1P2)
150
100
50
0
S1P
-
+
-
+
JTE-013
-
-
+
+

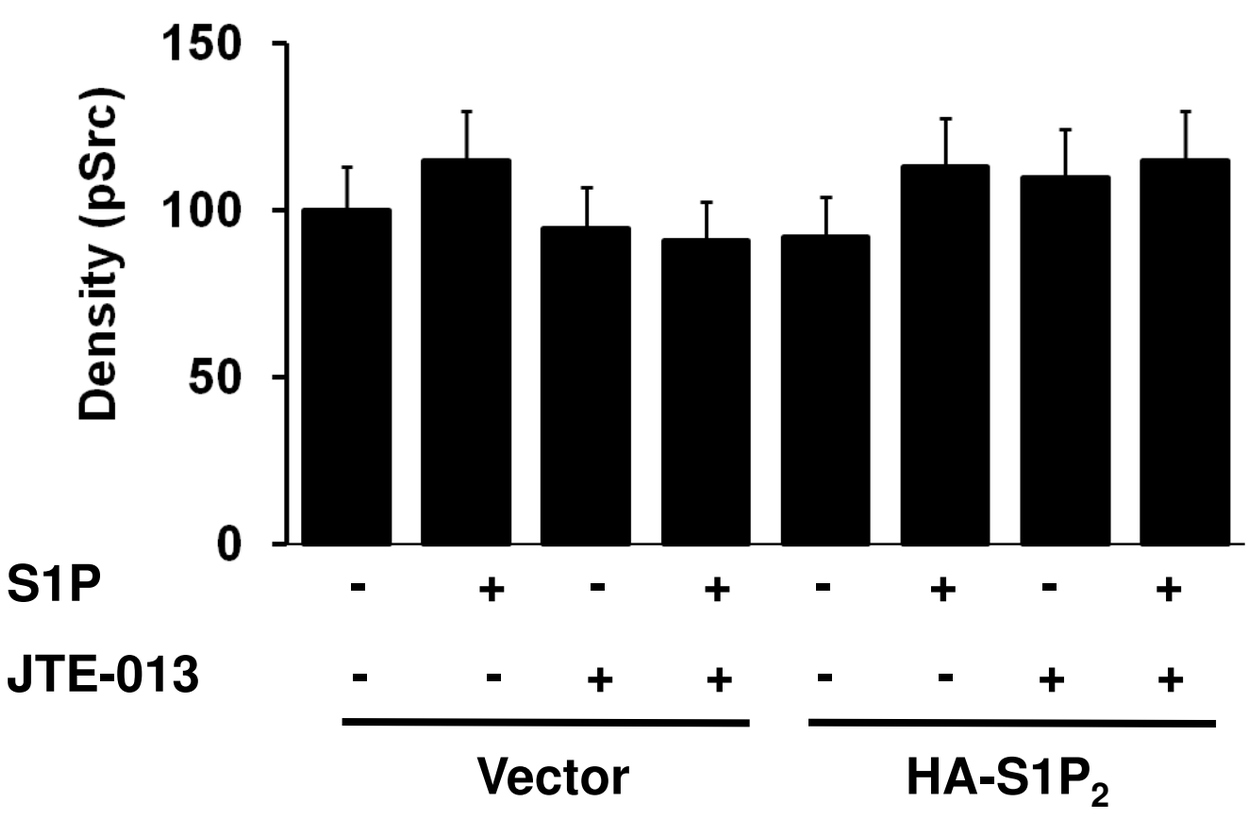
Density (pSrc)
150
100
50
0
S1P
-
+
-
+
-
+
-
+
JTE-013
-
-
+
+
-
-
+
+
Vector
HA-S1P2

Suppl.
Fig. 7A

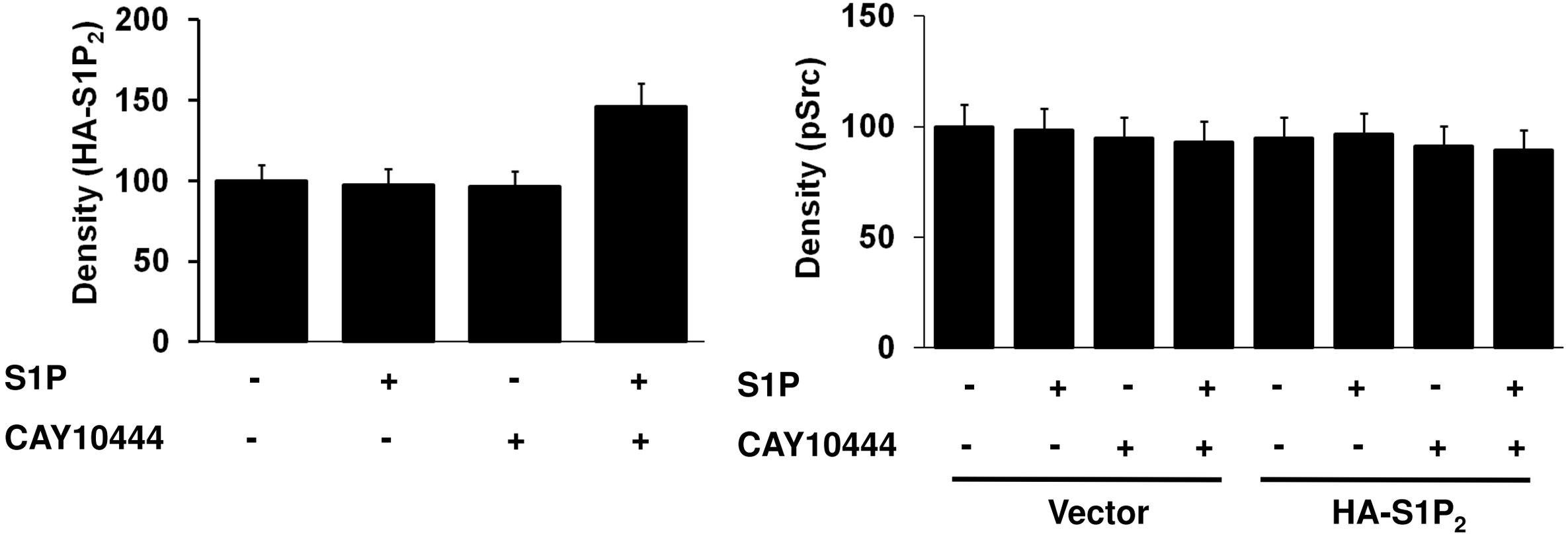
Density (HA-S1P2)
200
150
100
50
0
S1P
-
+
-
+
CAY10444
-
-
+
+
Density (pSrc)
150
100
50
0
S1P
-
+
-
+
-
+
-
+
CAY10444
-
-
+
+
-
-
+
+
Vector
HA-S1P2

Suppl.
Fig. 7B

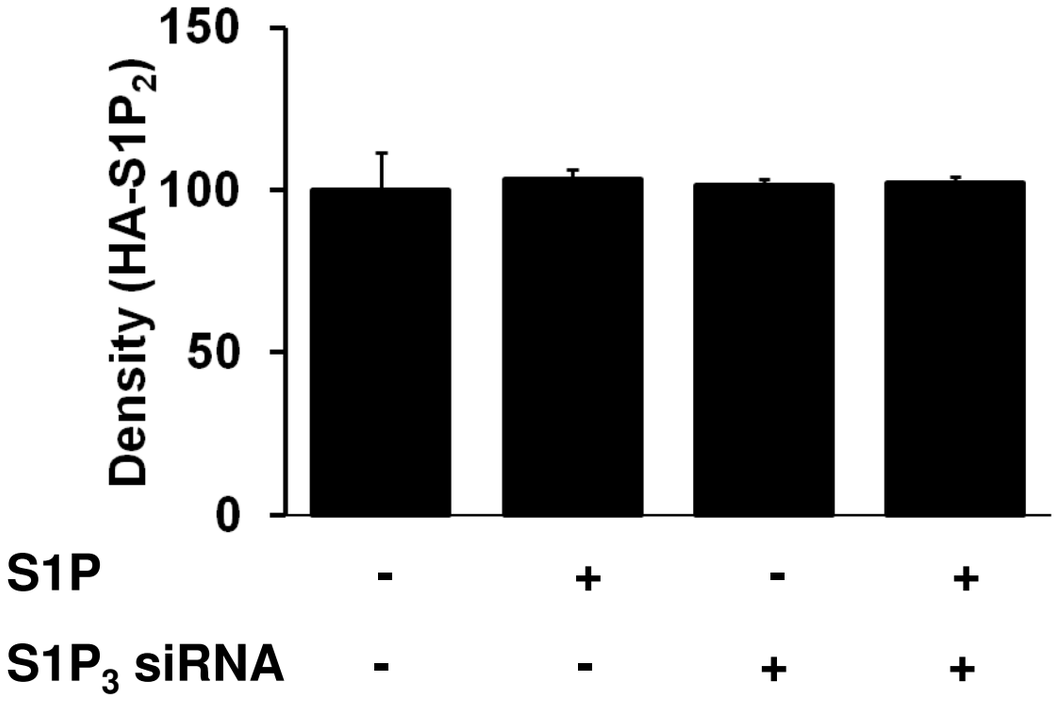
Density (HA-S1P2)
150
100
50
0
S1P
-
+
-
+
S1P3 siRNA
-
-
+
+

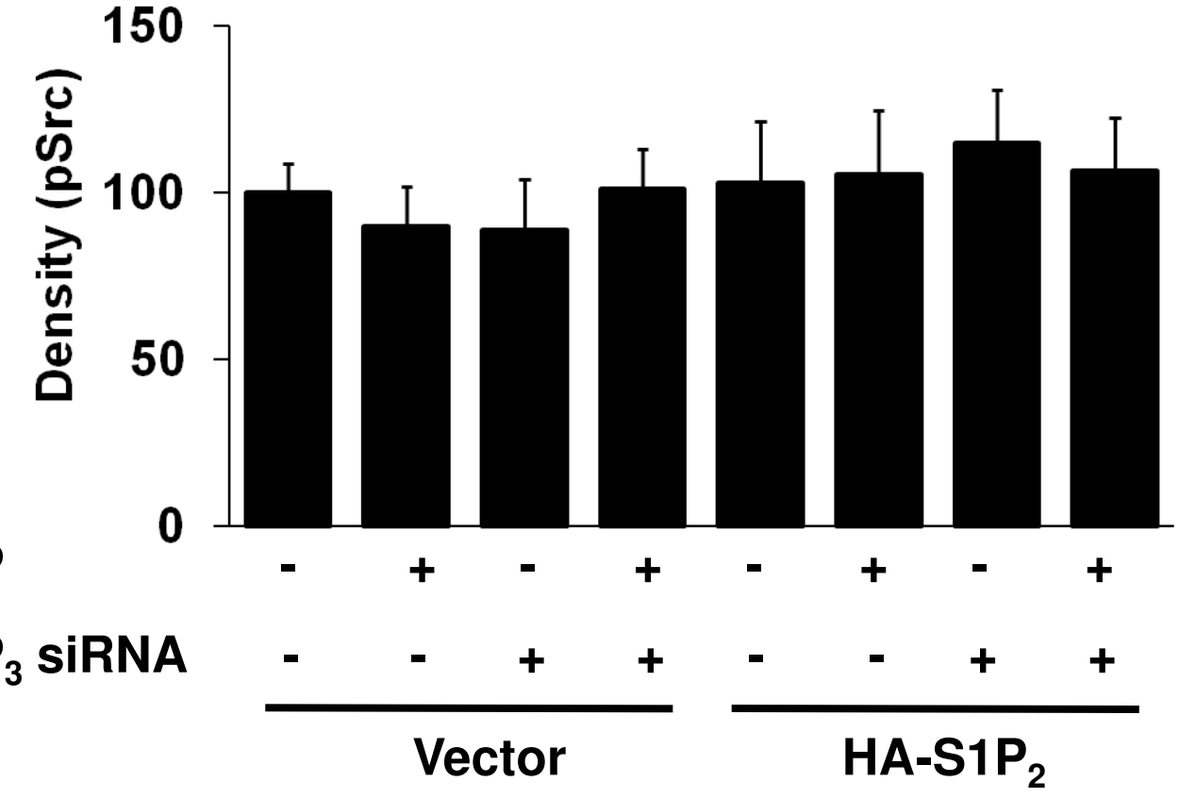
Density (pSrc)
150
100
50
0
S1P
-
+
-
+
-
+
-
+
S1P3 siRNA
-
-
+
+
-
-
+
+
Vector
HA-S1P2

Suppl.
Fig. 7C

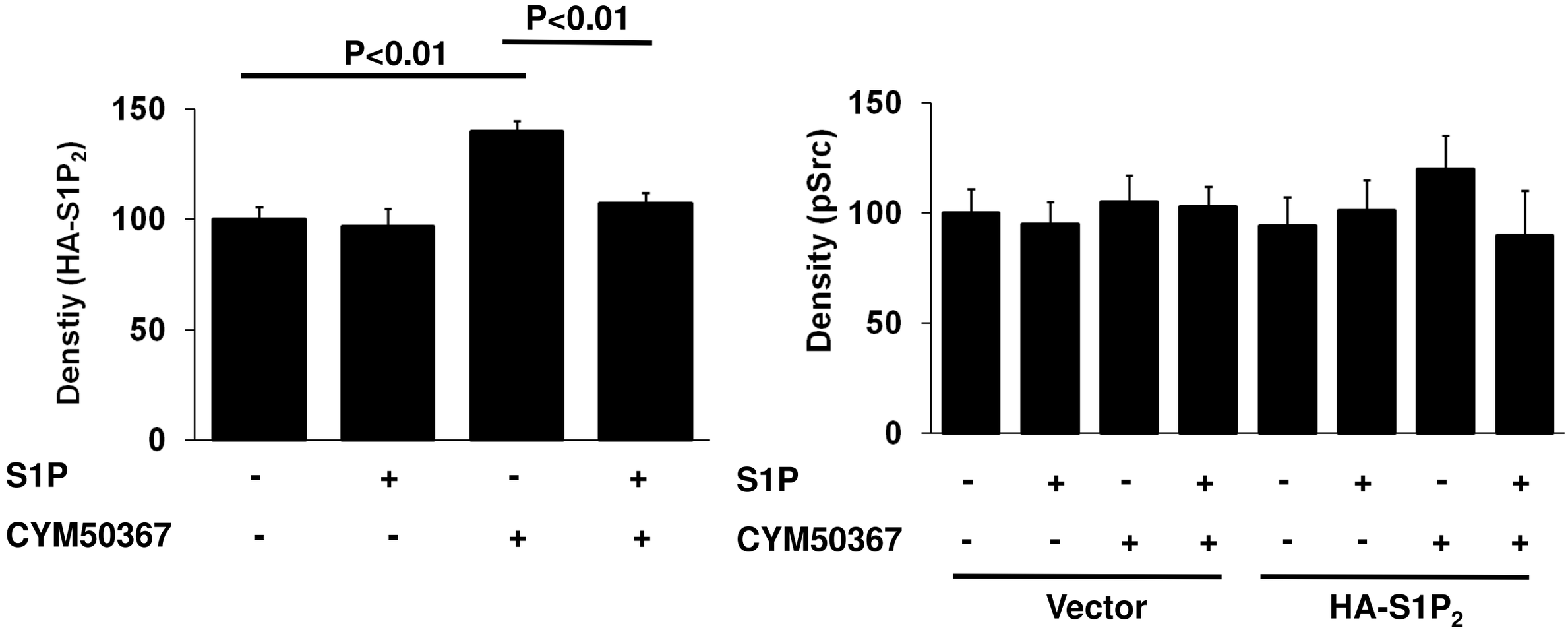
P<0.01
P<0.01
Denstiy (HA-S1P2)
150
100
50
0
S1P
CYM50367
-
+
Density (pSrc)
Vector
HA-S1P2

Suppl.
Fig. 7D

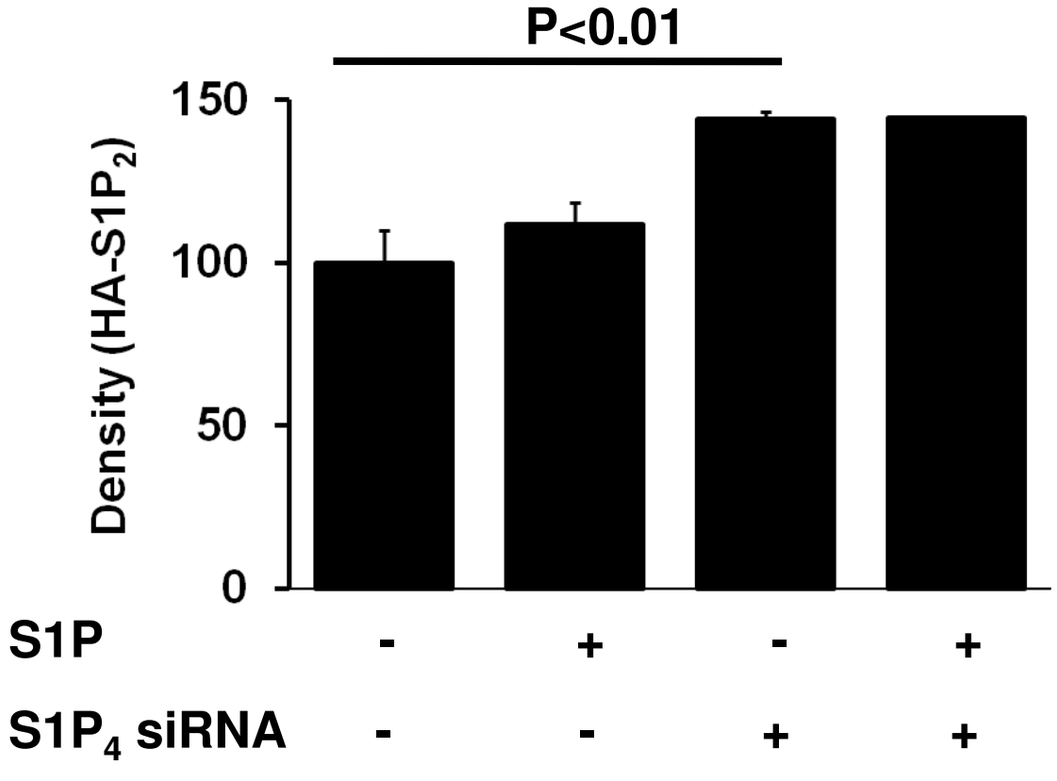
P<0.01
Density (HA-S1P2)
150
100
50
0
S1P
S1P4 siRNA
-
+
-
+
-
+
-
+

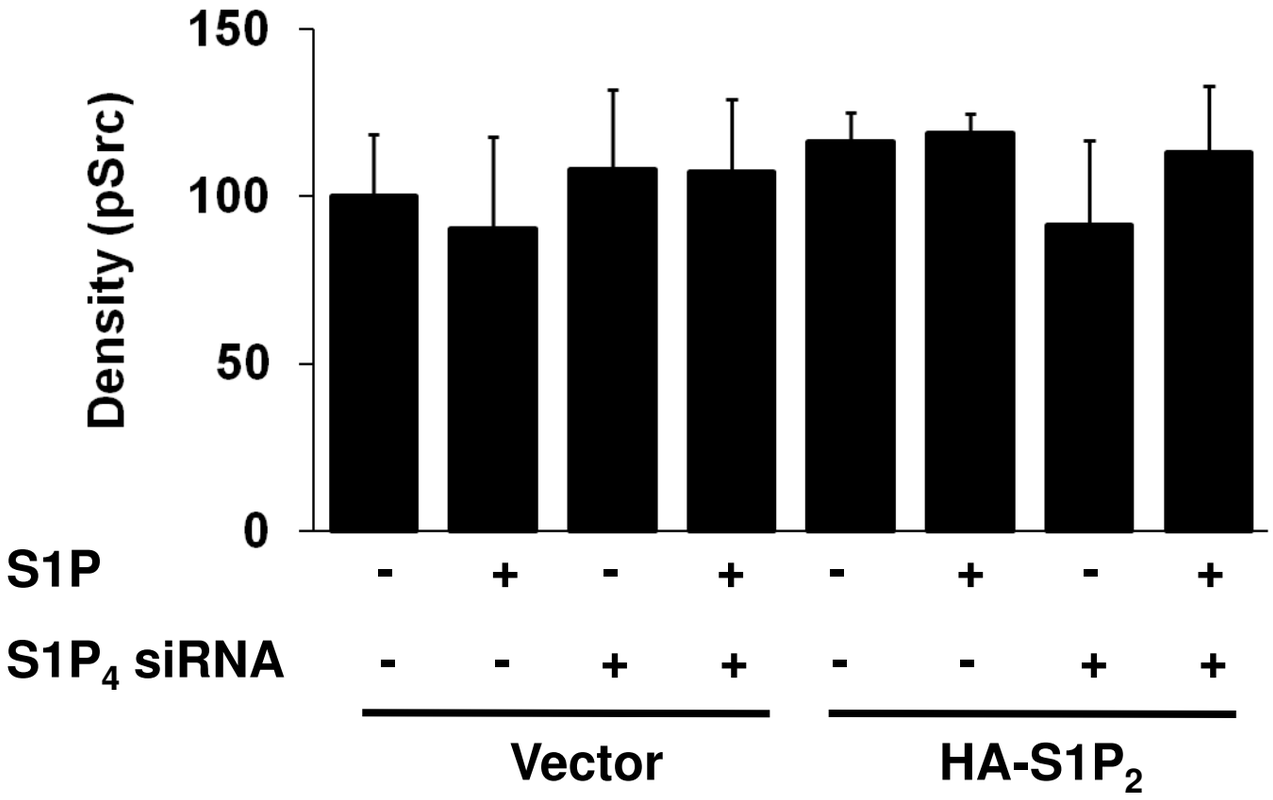
Density (pSrc)
150
100
50
0
S1P
S1P4 siRNA
-
+
-
+
-
+
-
+
-
+
-
+
-
+
-
+
Vector
HA-S1P2

Suppl.
Fig. 7E

Background: The role of the sphingosine 1-phosphate receptor-2 in cancer is controversial.

Results: Inhibition of sphingosine kinase 2/sphingosine 1-phosphate receptor-4 promotes nuclear translocation of sphingosine 1-phosphate receptor-2 and reduces cancer cell growth.

Conclusion: Sphingosine kinase 2 and sphingosine 1-phosphate receptor-4 participate to prevent sphingosine 1-phosphate receptor-2 nuclear localisation.

Significance: The sub-cellular localisation of sphingosine 1-phosphate receptor-2 determines cancer cell growth.